S1 Hunga Tonga-Hunga Ha'apai volcano impact Model Observation Comparison (HTHH-MOC) project: experiment protocol and model descriptions

Authors

Yunqian Zhu, Hideharu Akiyoshi, Valentina Aquila, Elisabeth Asher, Ewa M. Bednarz, Slimane Bekki, Christoph Brühl, Amy H. Butler, Parker Case, Simon Chabrillat, Gabriel Chiodo, Margot Clyne, Peter R. Colarco, Sandip Dhomse, Lola Falletti, Eric Fleming, Ben Johnson, Andrin Jörimann, Mahesh Kovilakam, Gerbrand Koren, Ales Kuchar, Nicolas Lebas, Qing Liang, Cheng-Cheng Liu, Graham Mann, Michael Manyin, Marion Marchand, Olaf Morgenstern, Paul A. Newman, Luke D. Oman, Freja F. Østerstrøm, Yifeng Peng, David Plummer, Ilaria Quaglia, William Randel, Samuel Rémy, Takashi Sekiya, Stephen Steenrod, Timofei Sukhodolov, Simone Tilmes, Kostas Tsigaridis, Rei Ueyama, Daniele Visioni, Xinyue Wang, Shingo Watanabe, Yousuke Yamashita, Pengfei Yu, Wandi Yu, Jun Zhang, Zhihong Zhuo

This supplement is a preprint of (with adjustment to the assessment style): Zhu et al. (2025).

Zhuo, Z., Wang, X., Zhu, Y., Yu, W., Bednarz, E. M., Fleming, E., Colarco, P. R., Watanabe, S., Plummer, D., Stenchikov, G., Randel, W., Bourassa, A., Aquila, V., Sekiya, T., Schoeberl, M. R., Tilmes, S., Zhang, J., Kushner, P. J., and Pausata, F. S. R.: Comparing multi-model ensemble simulations with observations and decadal projections of upper atmospheric variations following the Hunga eruption, *Atmos. Chem. Phys.*, 25, 13161–13176, https://doi.org/10.5194/acp-25-13161-2025, 2025.

Abstract

The 2022 Hunga volcanic eruption injected a significant amount of water vapour and a moderate amount of sulfur dioxide into the stratosphere, causing observable responses in the climate system. We have developed a model–observation comparison project to investigate the evolution of volcanic water and aerosols and their impacts on atmospheric dynamics, chemistry, and climate, using several state-of-the-art chemistry climate models. The project goals are (1) to evaluate the current chemistry–climate models to quantify their performance in comparison to observations and (2) to understand atmospheric responses in the Earth system after this exceptional event and investigate the potential impacts in the projected future. To achieve these goals, we designed specific experiments for direct comparisons to observations, for example from balloons and the Microwave Limb Sounder satellite instrument. Experiment 1 consists of two sets of free-running ensemble experiments from 2022 to 2031: one with fixed sea-surface temperatures and sea ice and one with coupled ocean. These experiments will help to understand the long-term evolution of water vapour and aerosols; quantify HTHH effects on stratospheric and mesospheric temperatures, dynamics, and transport; understand the impact of dynamic changes on ozone chemistry; quantify the net radiative forcings; and evaluate any surface climate impact. Experiment 2 is a nudged-run experiment from 2022 to 2023 using observed meteorology. To allow participation of more climate models with varying complexities of aerosol simulation, we include two sets of simulations in Experiment 2: Experiment 2a is designed for models with internally generated aerosol, while Experiment 2b is designed for models using prescribed aerosol surface area density. This experiment will help to analyse H_2O and aerosol evolution, quantify the net radiative forcings, understand the impacts on mid-latitude and polar O_3 chemistry, and allow close comparisons with observations.

S1.1 Introduction and motivations of this project

The Hunga Tonga–Hunga Ha'apai (HTHH) Impacts activity was established in the World Climate Research Programme (WCRP) Atmosphere Processes And their Role in Climate (APARC) as a limited-term focused cross-activity with a duration of 3 years. It aims to assess the impacts of the 15 January 2022 Hunga volcanic eruption and produce an assessment to document the Hunga impact on the climate system. The Hunga eruption injected an unprecedented amount of water (H_2O) and moderate sulfur dioxide (SO_2) into the stratosphere (Millán et al., 2022), presenting a unique opportunity to understand the impacts on the stratosphere of a large-magnitude explosive phreatomagmatic eruption. The wide range of satellite observations of the stratospheric water and sulfate plumes, global transport and dispersion of volcanic materials, and unusual chemical and temperature signals are helpful in assessing model representations of stratospheric chemistry, aerosol, and dynamics. For example, the Aura Microwave Limb Sounder (MLS) observed ~150 Tg of water injected by the Hunga eruption (Millán et al., 2022), which slowly decayed due to the polar stratospheric cloud (PSC) dehydration process and stratosphere–troposphere exchange (Fleming et al., 2024; Zhou et al., 2024). Large aerosol optical depth is observed by the Ozone Mapping and Profiler Suite (OMPS) (Taha et al., 2022), due to fast formation of sulfate (Zhu et al., 2022) and the high optical efficiency of Hunga aerosol particles (Li et al., 2024). Unlike the stratospheric warming patterns observed from previous large volcanic eruptions (El Chichón in 1982 and Pinatubo in 1991), global stratospheric temperatures decreased by 0.5 to 1.0 K in the first 2 years following the Hunga eruption, largely due to radiative cooling from injected water vapour (Randel et al., 2024). Satellite observations in June, July, and August 2022 reveal reduced lower-stratospheric ozone (O_3) over the Southern Hemisphere (SH) midlatitudes and subtropics, with high levels near the Equator, exceeding previous variability. These ozone anomalies coincide with a weakening of the Brewer–Dobson circulation during this period (Wang et al., 2023). Changes in stratospheric winds also influence the mesosphere, leading to a stronger mesospheric circulation and corresponding temperature changes (Yu et al., 2023). These observed phenomena provide a unique opportunity to test the ability of chemistry–climate models to simulate the evolution of volcanic aerosols combined with such a large amount of water vapour, as well as understand how volcanic water vapour and aerosols modify radiative balances and stratospheric ozone.

The APARC Hunga Impacts activity aims to provide a benchmark analysis of the eruption impacts so far and projections of eruption climate impacts over the next few years. Two multi-model evaluation projects are designed to facilitate the success of this activity: the Tonga Model Intercomparison Project (Tonga-MIP) (Clyne et al., 2024) and the Hunga

Tonga–Hunga Ha'apai Volcano Impact Model Observation Comparison (HTHH-MOC) project (this paper). The HTHH-MOC provides a foundation for a coordinated multi-model evaluation of global chemistry–climate models' performance in response to the Hunga volcanic eruption. It defines a set of perturbation experiments, where volcanic forcings – injected water vapour and aerosol concentrations – are consistently applied across participating model members. HTHH-MOC aims to assess how reliably global chemistry–climate models simulate the climate responses to this unprecedented volcanic forcing. This project enhances our confidence in attributing and interpreting observations following the Hunga eruption. The scientific questions related to the HTHH-MOC are as follows:

- How does the Hunga volcanic plumes' transport relate to or impact stratospheric dynamics (such as Brewer–Dobson circulation, polar vortex, and the quasi-biennial oscillation) and the upper atmosphere?
- What are the chemical impacts of the Hunga eruption in the stratosphere and mesosphere?
- What and how long is the radiative effect of the Hunga eruption?
- Does Hunga impact the tropospheric/surface climate?

Therefore, the HTHH-MOC project is focused on evaluating global chemistry–climate models regarding the following three science themes: (1) plume evolution, dispersion, and large-scale transport; (2) impacts on stratospheric chemistry and the ozone layer; and (3) radiative effect from the eruption and surface climate impacts. Besides the HTHH-MOC project, the assessment also includes analysis of observations and models that are not global climate models. In the following paragraph, we describe the HTHH-MOC experiment design and participating models.

S1.2 Experiment design

There are two experiments (Exp1 and Exp2 detailed below) designed to fulfill the scientific goals. Each experiment includes a set of simulations with different volcanic injections (i.e., with and without water and/or SO_2), to explore the separate impacts of volcanic water and aerosols during the post-eruption period: (a) control case (no eruption),(b) H_2O (~150 Tg) and SO_2 (0.5 Tg), (c) only H_2O (~150 Tg), and (d) only SO_2 (0.5 Tg). Simulations with the injection of SO_2 only (d) are optional and designed for aerosol-focused models. The SO_2 and water injections are prescribed based on Millán et al. (2022) and Carn et al. (2022). Note that~150 Tg of water is not the injection amount but the amount retained after the first couple of days. This is because some models form ice particles that fall out of the stratosphere due to large H2O supersaturation during the initial injection (Zhu et al., 2022); these models will have to inject more H_2O to counterbalance the ice formation (see Table S1.6). The only requirement is that the model should have reasonable comparison to the MLS observations for water vapour, as shown in Figure S1.1. Aside from retaining ~150 Tg of water, the water vapour enhancement should be near 10 to 50 hPa, and most of the water vapour should be located between 10°N and 30°S by March 2022.

The first experiment (Exp1) is a free-running ensemble simulation covering the period from 2022 to 2031. The experiment has been designed to answer questions on the following:

1. understanding the long-term evolution of Hunga water vapour and aerosols in free-running models;
2. quantifying Hunga effects on stratospheric temperatures, dynamics, and transport;
3. understanding the impact of dynamic changes on ozone chemistry;
4. quantifying the net radiative effects;
5. estimating surface impacts (e.g., temperature, El Niño–Southern Oscillation, monsoon precipitation).

Simulations with free-running meteorology are required to properly understand the impacts of the eruption on atmospheric dynamics and transport processes and the resulting impacts of those on chemical species (e.g., ozone) and surface climate. Since coupling of the atmosphere with ocean and land processes is required to fully simulate many aspects of the surface impacts, the use of coupled atmosphere, ocean, and land models is recommended. However, since such a fully interactive setup imposes additional computing requirements, an alternative model setup with fixed sea-surface temperatures (SSTs) and sea ice is also allowed. In that case, the prescribed climatological SSTs and sea-ice data are obtained by averaging SST during the past decade (2012–2021), with the same data imposed in both the H_2O + SO_2 (b) and control (a) simulations. It is important to note that

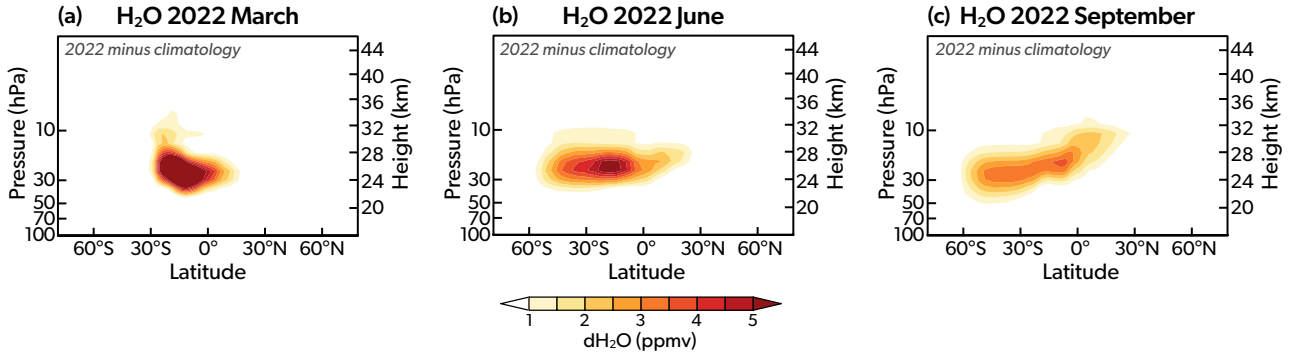

Figure S1.1: *Monthly average water vapour perturbation after the Hunga eruption from MLS. Panels (a)–(c) show the observed dispersion of the H_2O enhancement in 2022 in the months of (a) March, (b) June, and (c) September.*

both initial and boundary conditions in a model come with uncertainties, and model processes are simplified. Therefore, model simulations are influenced by the characteristics of the model itself and the background state of the atmospheric system (Jones et al., 2016; Brodowsky et al., 2021). To address some of the inherent uncertainties and reduce contribution of interannual variability to the forced response, we use a large ensemble of simulations with slightly varied initial conditions. Note that in the projection of stratospheric volcanic forcing, we only considered the Hunga eruption since 2022, and no future explosive eruptions are included. For example, the 2024 Mt. Ruang eruption contributed to elevated stratospheric aerosol optical depth, but it is not included. Particularly, the first 5 years of qualified model output of Exp1 is used to understand climate impacts on the mesosphere and ionosphere from 2022–2027, such as gravity wave drag, temperature changes, polar mesospheric clouds (PMCs), and atmospheric circulation. The qualified models need to resolve the upper atmosphere with vertical resolutions higher than or equal to what we request in Section S1.3.

Since some aspects of the response, e.g., impacts on the radiative effect, may be too noisy from free-running model simulations even with large ensembles, we have also designed the second experiment, which uses nudged temperature and meteorology to ensure that the meteorology will be as close as possible to the one observed and thus isolate chemical changes and their radiative effect. Experiment 2 (Exp2) is a 2-year simulation that runs from 2022 to 2023 with nudged winds and/or temperature to answer questions on H_2O and aerosol evolution, quantification of the net radiative effects, and impacts on mid-latitude and polar ozone chemistry. Exp2 has two distinct realisations: Experiment 2a (Exp2a) and Experiment 2b (Exp2b). The models participating in Exp2a all have a prognostic aerosol module but vary in the complexity of their representation of aerosol microphysics (i.e., bulk, modal, or sectional). Models participating in Exp2b use prescribed aerosol surface area density (SAD) and radiative properties as input to the models (Jörimann et al., 2025). The prescribed aerosol properties are calculated using Global Space-based Stratospheric Aerosol Climatology (GloSSAC; Thomason et al., 2018; Kovilakam et al., 2020; Kovilakam et al., 2023) version 2.22 aerosol data from 1979–2023. Note that for the period after the Hunga eruption, GloSSAC uses the Stratospheric Aerosol and Gas Experiment (SAGEIII/ISS) version 5.3 interpolated along the time axis and the Optical Spectrograph and InfraRed Imager System (OSIRIS) version 7.3 to fill in any missing data poleward of 60°N/S due to the unavailability of the Cloud-Aerosol Lidar and Infrared Pathfinder Satellite Observations (CALIPSO) data since January 2022. Therefore, when conducting analyses north/south of 60°N/S it should be noted that the aerosols may be underestimated due to the OSIRIS instrument retrieval biases. We ask for the models to check their initial chemical fields against the MLS to see if the models are qualified to evaluate their ozone chemistry. The nudged runs of Exp2 enable isolation of the chemical impact of the Hunga eruption from the volcanically induced changes in dynamics by comparing the runs with and without H_2O + SO_2 injection. The net radiative effect anomaly due to water and sulfate aerosol can also be calculated by comparing the control run (a) with the H_2O + SO_2 injection run (b).

Table S1.1 shows the forcings and emissions data used for the HTHH-MOC experiments. Table S1.2 shows the settings specific to each experiment. For volcanic injection for Exp1 and 2, we recommend the injections of H_2O and SO_2 at 04:00 UTC on 15 January 2022. All the models are required to retain

a similar amount of water as observed by the MLS (~150 Tg). The models are recommended to compare with the MLS evolution for validation (Figure S1.1). The goal is to retain the same amount of water and similar altitude to start with, so we can analyse the water's impact on the stratosphere and climate. If injecting 25–30 km cannot retain 150 Tg, models can inject higher than 30 km. The SO_2 injection is required to be 0.5 Tg for all models. The injection locations are not required to be co-injected with H_2O.

The data analysis of this project is designed to do inter-model comparisons, as well as inter-experiment comparisons. For example, the comparisons between Exp2a and Exp2b can help to understand how well we simulate the sulfate SAD and the importance of SAD variation for stratospheric ozone chemistry. Comparing Exp1 and Exp2 for the same period can help understand instantaneous and adjusted radiative effects. In addition, large (10–20) member ensembles are requested for free-running simulations to better quantify the role of internal variability in the climate response.

A parallel model intercomparison project, Tonga-MIP (Clyne et al., 2024), will also be part of the 2025 Hunga assessment. It is designed to explore the plume evolution between 1 day and up to 1–2 months after the eruption. Tonga-MIP was initiated before the APARC Hunga activity started. It will be described in a separate paper, but we list it here to document the comprehensiveness of the modelling effort for the Hunga assessment. Two objectives of Tonga-MIP cannot be achieved by Exp1 and Exp2:

1. The nudged experiment of Tonga-MIP aims to intercompare the microphysical processes (i.e., cloud and aerosol physics and sulfur chemistry) between different models. Therefore, all models are requested to inject 150 Tg of water, but the retained amount of water varies between models, differing from Exp1 and Exp2, which require retaining ~150 Tg of water in the stratosphere. The SO_2 injection is 0.5 Tg, the same as in the HTHH-MOC experiments. The injections are required to occur between 25–30 km altitude, within the latitude and longitude box of 22–14° S and 182–186° E, at a constant vertical volume mixing ratio for 6 h starting at 04:00 UTC on 15 January 2022.
2. The free-running experiment of Tonga-MIP aims to study the radiative effect of water and SO_2 on the Hunga plume's descending and ascending behaviour during the first month after the eruption, since the Hunga water and aerosol plumes were observed to descend several kilometres during the first month after the eruption (Sellitto et al., 2022; Randel et al., 2024). Therefore, Tonga-MIP is designed to nudge the atmosphere up until several different dates and then explore the plume-descending patterns in free-running mode after those dates. The selected dates are 21, 26, and 31 January 2022. Most of the models that participate in Tonga-MIP also participate in the HTHH-MOC.

S1.3 Model output

The model output covers variables based on the Chemistry–Climate Modeling Initiative (CCMI) output list, with some additions specific to this study. The detailed list is provided in `https://doi.org/10.5194/gmd-18-5487-2025-supplement`. All participating models are requested to generate the same variable names, units, and ordering of dimensions (longitude from 0 to 360° E, latitude from 90° S to 90° N, and pressure levels from 1000 to 0.03 hPa, or altitude from 0 to 73 000 m), as well as consistent file name structures, such as `variable_domain_modelname_experimentname.nc` or `domain_modelname_experimentname.variable.nc`. Examples of `Experiment_name` are `HTHHMOC-Exp1` and `HTHHMOC-Exp2`. Example file names include `Monthlymean_WACCM6MAM_HTHHMOC-Exp1-NoVolc-fixedSST.ensemble001.O3.nc` or `O3_Dailymean_WACCM6MAM_HTHHMOC-Exp1-H2Oonly-CoupledOcean.ensemble001.nc`.

The 3-D model output is requested both on native model levels (hybrid pressure or height) and interpolated to the CMIP6 `plev39` grid (`plev39`: 1000, 925, 850, 700, 600, 500, 400, 300, 250, 200, 170, 150, 130, 115, 100, 90, 80, 70, 50, 30, 20, 15, 10, 7, 5, 3, 2, 1.5, 1.0, 0.7, 0.5, 0.4, 0.3, 0.2, 0.15, 0.1, 0.07, 0.05, 0.03 hPa), and, for mesospheric analysis, additional levels are added: 0.02, 0.01, 0.007, 0.005, 0.003, and 0.001 hPa above the plev39 grid.

Monthly mean output is requested for all variables in Exp1, with some fields (as specified in the accompanying Excel sheet) requested as daily means. Some daily mean variables are limited to surface fields or to a reduced number of pressure levels. Daily mean output is requested for all variables in Exp2.

The total model output (approximately 33 TB) from Exp1 and Exp2 is archived at the JASMIN workspace (`https://jasmin.ac.uk/`, last access: 12 August 2025). JASMIN provides large storage capacity

Table S1.1: *Summary of forcings and emissions data used in HTHH-MOC experiments.*

Category	Description
Spin-up*	5-year nudged runs.
Degassing and eruptive volcano source**	Need both degassing and eruptive volcanic input for 5-year spin-up. Degassing continues during the experiment runs (e.g. 10 years for Exp1, 2 years for Exp2). recommended references: Volcanic degassing (Carn et al., 2016; Carn et al., 2017); Eruptive volcanoes (Neely III and Schmidt 2016 `https://archive.researchdata.leeds.ac.uk/96/` or Carn et al. 2017; Assume no more explosive volcanoes after Hunga.
Surface emission	Coupled Model Intercomparison Project phase 6 (CMIP6) emissions follow SSP2-4.5 (Gidden et al., 2019), which adopts an intermediate greenhouse gas (GHG) emission: CO_2 emissions around current levels before beginning to decline by 2050.
Chemical initialisation	Stratospheric chemistry fields (e.g., O_3, H_2O) at the beginning of 2022 should be compared with MLS observations for validation if the model participates in evaluation of the Hunga stratospheric chemistry impact.

* Five years are sufficient to reach sulfate equilibrium in the stratosphere; water may require up to 7 years (each model may adjust spin-up time based on its configuration).

** Recommended degassing volcanic emissions are injected at the cone altitude with constant flux based on Carn et al. (2017). Database is updated through 2022 here: `https://doi.org/10.5067/MEASURES/SO2/DATA406`.

Table S1.2: *Experiment design for the HTHH-MOC simulations.*

Experiment	Meteorology	Period	Aerosol Treatment	QBO	SST Configuration	Ensemble Members
Exp1.FixedSST	Free run starts 1 Feb (nudged until 31 Jan).	2022–2031 (10 years; first 5 years for mesospheric analysis).	Model-simulated aerosol or prescribed.	Internally generated (nudge if model does not generate).	Fixed climatology = mean of monthly averages 2012–2021, repeating annually. This applies to spin-up time as well.	10–20
Exp1.CoupledOcean	Free run starts 1 Feb (nudged until 31 Jan).	2022–2031 (10 years; first 5 years for mesospheric analysis).	Model-simulated aerosol or prescribed.	Internally generated (nudge if model does not generate).	Coupled ocean (optional); initialise with observed ocean state (see Section S1.4 for model descriptions).	10–20
Exp2a	Nudged wind only and/or nudged T and wind*.	2022–2023 (2 years).	Model-simulated aerosol.	Nudged.	Observed SST.	1
Exp2b	Nudged wind only and/or nudged T and wind*.	2022–2023 (2 years).	Prescribed.	Nudged.	Observed SST.	1

* "Nudged T and wind" indicates specified-dynamics (SD) configurations in which temperature and/or wind fields are relaxed toward reanalysis data. Coupled configurations are optional depending on individual model capability.

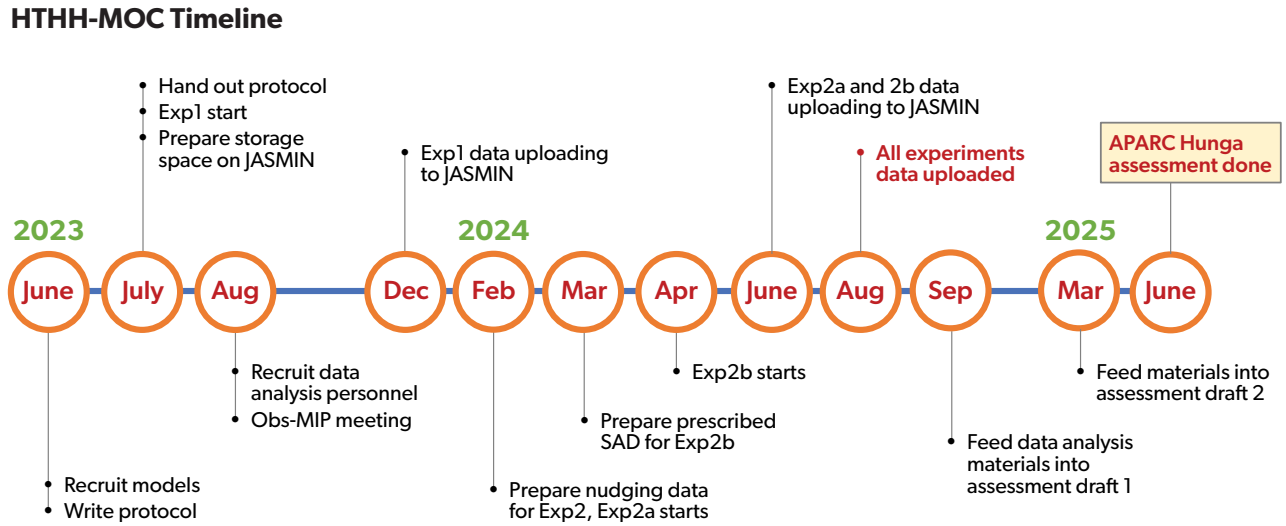

Figure S1.2: *Timeline designed for the HTHH-MOC project to coordinate with the APARC Hunga Impact assessment.*

and computing resources to facilitate data archiving and post-processing analysis for this project. This setup reduces the need for data transfers and allows reproducible computational workflows. Seddon et al. (2023) describe the facility in detail. The next project phase will publicly release the data by transferring it to the Centre for Environmental Data Analysis (CEDA) archiving system.

S1.4 Model descriptions and the Hunga volcanic injection specification

As part of the 3-year Hunga Impact activity, this project is highly time-sensitive. We designed the timeline for each experiment (Figure S1.2) to facilitate the completion of the 2025 Hunga Impact assessment. However, the JASMIN workspace will remain open for the uploading of modelling data after the deadline denoted in Figure S1.2 until 2025.

This paper only includes model descriptions for those models that submitted the output following the assessment timeline. The model setup follows the protocols listed in Section S1.2 unless specified below. Tables S1.3 to S1.6 provide key information on the participant models, which are described in detail in the following paragraphs for each model.

Table S1.3: *Participating models and contact information for HTHH-MOC and Tonga-MIP.*

Model name	Description reference paper	Developing institutions	Primary contact
CAM5/CARMA	Yu et al. (2015)	CU Boulder; Jinan Univ.	Pengfei Yu (pengfei.yu@colorado.edu); Yifeng Peng (pengyf16@lzu.edu.cn)
CCSRNIES-MIROC3.2	Akiyoshi et al. (2023) and Akiyoshi et al. (2016)	NIES	Yousuke Yamashita (yamashita.yosuke@nies.go.jp); Hideharu Akiyoshi (hakiyosi@nies.go.jp)
CMAM	Jonsson et al. (2004) and Scinocca et al. (2008)	CCCma, ECCC	David Plummer (david.plummer@ec.gc.ca)
EMAC MPIC	Schallock et al. (2023)	MPI-C, MPI-M, DLR	Christoph Brühl (christoph.bruehl@mpic.de)
GA4 UM-UKCA	Dhomse et al. (2020)	Univ. Leeds	Graham Mann (G.W.Mann@leeds.ac.uk); Sandip Dhomse (S.S.Dhomse@leeds.ac.uk)
GEOSCCM	Nielsen et al. (2017)	NASA	Peter Colarco (peter.r.colarco@nasa.gov)
GEOS/CARMA	Nielsen et al. (2017)	NASA	Parker Case (parker.a.case@nasa.gov)
GSFC2D	Fleming et al. (2024)	NASA	Eric Fleming (eric.l.fleming@nasa.gov)
IFS-COMPO Cy49R1	Huijnen et al. (2016) and Rémy et al. (2022)	ECMWF; team CAMS2_35	Simon Chabrillat (Simon.chabrillat@aeronomie.be); Samuel Rémy (sr@hygeos.com)
LMDZ6.2-LR-STRATAER / LMDZ6.2-LR-STRATAER-REPROBUS	Boucher et al. (2020) and Marchand et al. (2012)	CNRS, Sorbonne Univ., IPSL, LATMOS, LOCEAN	Marion Marchand (marion.marchand@latmos.ipsl.fr); Slimane Bekki (slimane.bekki@latmos.ipsl.fr); Nicolas Lebas (nicolas.lebas@locean.ipsl.fr); Lola Falletti (lola.falletti@latmos.ipsl.fr)
MIROC-CHASER	Sekiya et al. (2016)	JAMSTEC	Shingo Watanabe (wnabe@jamstec.go.jp); Takashi Sekiya (tsekiya@jamstec.go.jp)
MIROC-ES2H	Tatebe et al. (2019) and Kawamiya et al. (2020)	JAMSTEC; NIES	Shingo Watanabe (wnabe@jamstec.go.jp); Takashi Sekiya (tsekiya@jamstec.go.jp); Tatsuya Nagashima (nagashima.tatsuya@nies.go.jp); Kengo Sudo (kengo@nagoya-u.jp)
SOCOLv4	Sukhodolov et al. (2021)	PMOD/WRC; ETH-Zurich	Timofei Sukhodolov (timofei.sukhodolov@pmodwrc.ch)
UKESM1.1	Sellar et al. (2019), Sellar et al. (2020) and Dennison et al. (2019)	UK Met Office; UK Universities; NCAS	Graham Mann (g.w.mann@leeds.ac.uk); Sandip Dhomse (s.s.dhomse@leeds.ac.uk); Ben Johnson (ben.johnson@metoffice.gov.uk); Mohit Dalvi (mohit.dalvi@metoffice.gov.uk); Luke Abraham (nla27@cam.ac.uk); James Keeble (j.keeble2@lancaster.ac.uk)
WACCM6/CARMA	Tilmes et al. (2023)	NCAR	Simone Tilmes (tilmes@ucar.edu); Cheng-Cheng Liu (chengcheng.liu@lasp.colorado.edu); Yunqian Zhu (yunqian.zhu@noaa.gov); Margot Clyne (Tonga-MIP, margot.clyne@colorado.edu)
WACCM6/MAM	Mills et al. (2016)	NCAR	Xinyue Wang (xinyuew@colorado.edu); Simone Tilmes (tilmes@ucar.edu); Jun Zhang (jzhan166@ucar.edu); Wandi Yu (yu44@llnl.gov); Zhihong Zhuo (zhuo.zhihong@uqam.ca); Ewa Bednarz (ewa.bednarz@noaa.gov); Margot Clyne (Tonga-MIP, margot.clyne@colorado.edu)

CAM5/CARMA

The atmospheric component of the Community Atmosphere Model version 5 (CAM5; Lamarque et al. 2012) is the atmospheric component of the Community Earth System Model, version 1 (CESM1.2.2; Hurrell et al. 2013), with a top at around 45 km. CAM5 has a horizontal resolution of 1.9° latitude × 2.5° longitude, utilising the finite-volume dynamical core (Lin and Rood, 1996). The model has 56 vertical levels, with a vertical resolution of approximately 1 km in the upper troposphere and lower stratosphere.

The modeled winds and temperatures were nudged to the 3 h Goddard Earth Observing System 5 (GEOS-5) reanalysis dataset (Molod et al., 2015) every time step (30 min) by 1 % (i.e., a 50 h Newtonian relaxation timescale). The aerosol is interactively simulated using a sectional aerosol microphysics model, CARMA (Community Aerosol and Radiation Model for Atmospheres; Yu et al. 2015). The model uses the Model for Ozone and Related Chemical Tracers (MOZART) chemistry that is used for both tropospheric (Emmons et al., 2010) and stratospheric chemistry (English et al., 2011; Mills et al., 2016). The volcanic emissions from continuously degassing volcanoes use the emission inventory RCP8.5 and FINNv1.5. No volcanic eruptions except the Hunga 2022 eruption are included.

The initial volcanic injection altitude and area are determined by validating the water and aerosol transportation in months shown in S1.1 following the tests in Zhu et al. (2022), Wang et al. (2023), and Zhang et al. (2024). In these simulations, the H2O is injected at 25 to 35 km altitude, and SO2 is injected at 20 to 28 km altitude. The injection latitude ranges from 22 to 14° S, and longitude ranges from 182 to 186° E (Zhu et al., 2022). The initial injection of H2O is 150 Tg, with approximately 135 Tg left after the first week following the eruption.

CCSRNIES-MIROC3.2

The Center for Climate System Research / National Institute for Environmental Studies–Model for Interdisciplinary Research on Climate version 3.2 Chemistry–Climate Model (CCSRNIES-MIROC3.2 CCM; Akiyoshi et al. 2023) is based on version 3.2 of the MIROC atmospheric general circulation model (AGCM), incorporating a stratospheric chemistry module developed at the National Institute for Environmental Studies (NIES) and the University of Tokyo. The model has a horizontal resolution of T42 (2.8° latitude × 2.8° longitude) and 34 vertical levels, with a vertical resolution of approximately 1 km in the lower stratosphere–upper troposphere and 3 km in the upper stratosphere and mesosphere. The model top is located at 0.01 hPa (approximately 80 km).

The chemistry in the CCSRNIES-MIROC3.2 CCM is a stratospheric chemistry module including 42 photolysis reactions, 142 gas-phase chemical reactions, and 13 heterogeneous reactions for multiple aerosol types (Akiyoshi et al., 2023). Tropospheric chemistry is not included, but the stratospheric chemistry scheme is used for both the troposphere and the mesosphere. In the CCSRNIES-MIROC3.2 CCM, only Exp2b can be performed. The atmospheric temperature and horizontal winds are nudged toward Modern-Era Retrospective analysis for Research and Applications Version 2 (MERRA-2) reanalysis (Gelaro et al., 2017) with a 1-day relaxation using instant values at 6-hour intervals (Akiyoshi et al., 2016). The HadISST data are used during the simulation.

The CCSRNIES-MIROC3.2 CCM does not have any microphysics scheme for volcanic aerosols. The surface area and spectral optical parameters of extinction, single scattering albedo, and asymmetric factor for Hunga aerosols were prescribed in the model from the GloSSAC version 2.22 aerosol data (Jörimann et al., 2025). H2O was injected instantly on 15 January 2022 at the 12 grids of the model in the region 181.4–187.0° E in longitude, 14.0–22.3° S in latitude, and 12.0–27.6 hPa in pressure level. A uniform number density of 1.709×10^{15} molec. cm^{-3} H_2O was injected in each of the 12 grids, which amounts to approximately 150 Tg.

CMAM

The Canadian Middle Atmosphere Model (CMAM) is based on a vertically extended version of CanAM3.1, the third-generation Canadian Atmospheric Model (Scinocca et al., 2008). Compared to the standard configuration of CanAM3.1, for CMAM the model top was raised to 0.0006 hPa (approximately 95 km), and the parameterisation of non-orographic gravity wave drag (Scinocca, 2003) and additional radiative processes important in the middle atmosphere (Fomichev et al., 2004) have been included.

The gas-phase chemistry includes a comprehensive description of the inorganic O_x, NO_x, HO_x, ClO_x, and BrO_x families, along with CH_4, N_2O, six chlorine-containing halocarbons, CH_3Br and, to account for an additional 5 ppt of bromine from short-lived source gases, CH_2Br_2 and $CHBr_3$ (Jonsson et al., 2004). A prognostic description of, and associated heterogeneous chemical reactions on, water ice PSCs (PSC Type II) and liquid ternary solution (PSC Type Ib) particles

Table S1.4: *Participating models in HTHH-MOC and Tonga-MIP.*

Model names	Exp1.FixedSST	Exp1.CoupledOcean	Exp2a	Exp2b	Tonga-MIP (Clyne et al. 2024)
CAM5/CARMA			**X**		
CCSRNIES-MIROC3.2				**X**	
CMAM	**X** (H_2O-only)(*)				
EMAC MPIC			**X**		
GA4 UM-UKCA					**X**
GEOSCCM	**X**		**X**		**X**
GEOS/CARMA			**X**		
GSFC2D	**X**(*)			**X**	
IFS-COMPO			**X**		
LMDZ6.2-LR-STRATAER			**X**		**X**
LMDZ6.2-LR-STRATAER-REPROBUS			**X**		**X**
MIROC-CHASER	**X**		**X**		
MIROC-ES2H					**X**
SOCOLv4					**X**
UKESM1.1			**X**		**X**
WACCM6/CARMA			**X**		**X**
WACCM6/MAM	**X**(*)	**X**(*)	**X**		**X**

* Models qualified to analyse mesospheric components are marked with an asterisk.

is included, although gravitational settling (dehydration or denitrification) is not calculated, and species return to the gas phase when conditions no longer support the existence of PSC particles.

The simulations for the HTHH-MOC simulations were performed at T47 spectral resolution (approximately 3.8° resolution on the linear transform grid used for the model physics), with 80 vertical levels giving a vertical resolution of approximately 0.8 km at 100 hPa, increasing to 2.3 km above 0.1 hPa. The CMAM does not internally generate a QBO, so the zonal winds in the equatorial region were nudged towards a dataset based on observed variations up to December 2023, constructed using the method ofNaujokat (1986) and extended into the future by repeating a historical period that is congruent with the observed QBO in late 2023. Water vapour from the Hunga eruption was added as a zonally averaged perturbation to the model water over 5 days from 00:00 UTC on 20 February 2022. The spatial distribution of the anomaly was designed to reproduce the water vapour anomaly observed in mid-February by the Atmospheric Chemistry Experiment – Fourier Transform Spectrometer (ACE-FTS) (Bernath et al., 2005) satellite (Patrick Sheese, personal communication, 2022), with a maximum value of 13.3 ppm at 17°S and 25.5 km and producing an anomaly of ~150 Tg H_2O in the stratosphere.

EMAC MPIC

The chemistry–climate model EMAC (ECHAM5/MESSy Atmospheric Chemistry) consists of the European Centre Hamburg general circulation model (ECHAM5) and the Modular Earth Submodel System (MESSy) (e.g., Jöckel et al., 2010). Here we use the version of Schallock et al. (2023) in horizontal resolution T63 (1.87° × 1.87°) with 90 levels between the surface and 0.01 hPa.

Vorticity, divergence, and temperatures between surface and 100 hPa are nudged to the ERA5 reanalysis of ECMWF (Hersbach et al., 2020), as well as surface pressure. SSTs and sea ice cover are prescribed by ERA5 data. The model can generate an internal QBO, but for comparison with observations it was slightly nudged to the Singapore data compiled by the Free University of Berlin and Karlsruhe Institute

Table S1.5: *Model resolutions and schemes used for HTHH-MOC experiments.*

Model names	Horizontal resolution	nlevels	Model Top	Vertical resolution in the stratosphere	Aerosol scheme	Specified dynamic source	QBO (free run)	Chemistry package (tropospheric chemistry?)
CAM5/CARMA	~2°	56	45 km	1–4 km	CARMA sectional (20 bins)	GEOS-5	–	MOZART (yes)
CCSRNIES-MIROC3.2	T42	34	0.01 hPa	1–3 km	None	MERRA-2	–	full strat; no tropo
CMAM	T47	80	0.0006 hPa	0.8–2.5 km	None	ERA-5	nudged	strat + CH_4–NOx (tropo)
EMAC MPIC	T63	90	0.01 hPa	0.5 km in LS	GMXE (modal)	ERA-5	–	MECCA (simplified tropo)
GEOSCCM	c90 (~1°)	72	0.01 hPa	~1 km	GOCART (Bulk)	MERRA-2/GEOS-FP	Internal	GMI (yes)
GEOS/CARMA	c90 (~1°)	72	0.01 hPa	~1 km	CARMA (sectional 24 bins)	MERRA-2/GEOS-FP	–	GMI (yes)
GSFC2D	4°	76	0.002 hPa (~92 km)	1 km	Prescribed only	MERRA-2	Internal	full strat; partial trop
IFS-COMPO	T_L511 (~40 km)	137	0.01 hPa	0.5–1.5 km	Bulk	ERA-5	–	BASCOE (strat) + CB05 (tropo)
LMDZ6.2-LR-STRATAER	2.5° × 1.3°	79	80 km	1–5 km	S3A (sectional 36 bins)	ERA-5	–	No
LMDZ6.2-LR-STRATAER-REPROBUS	2.5° × 1.3°	79	80 km	1–5 km	S3A (sectional 36 bins)	ERA-5	–	REPROBUS
MIROC-CHASER	T85	81	0.004 hPa	0.7–1.2 km	MAM3	MERRA-2	Internal	tropo-strato chemistry
UKESM1.1	N96	85	80 km	0.6–0.7 km in LS	GLOMAP-mode	ERA-5	Internal	CheST (strat-trop chem.)
WACCM6/CARMA	~1°	70	140 km	1–2 km	Sectional (20 bins)	MERRA-2	–	MOZART (yes)
WACCM6/MAM	~1°	70	140 km	1–2 km	MAM4	MERRA-2	Internal	MOZART (yes)

of Technology (Giorgetta et al., 2006).

The model contains gas-phase and heterogeneous chemistry on PSCs and interactive aerosols. Surface mixing ratios of chlorine- and bromine-containing halocarbons and other long-lived gases are nudged to Advanced Global Atmospheric Gases Experiment (AGAGE) observations. The microphysical modal aerosol module contains four soluble and three insoluble modes for sulfate, nitrate, dust, organic and black carbon, and aerosol water (Pringle et al., 2010). The instantaneous radiative effect by tropospheric and stratospheric aerosols can be calculated online by multiple calls of the radiation module.

Volcanoes injecting material into the stratosphere are considered as in Schallock et al. (2023) using the perturbations of stratospheric SO_2 observed by the Michelson Interferometer for Passive Atmospheric Sounding (MIPAS) and aerosol extinction observed by OSIRIS. This method, based typically on data of a 10-day period, distributes the injected SO2 over a larger volume than typical point source approaches using the same integrated mass (see also Kohl et al., 2025). For Hunga this method has the disadvantage that H_2O and SO_2 are not co-injected since H_2O is injected over a 12-hour period as a slab consisting of four horizontal boxes and a Gaussian vertical distribution centred at 21.5 hPa. For Exp2a we continue the 30-year transient simulation presented in Schal-

Table S1.6: *Hunga volcanic injection profile for HTHH-MOC experiments.*

Model names	Date and duration	H_2O amount (after 1 week)	H_2O altitude	H_2O location / area	SO_2 amount	SO_2 altitude	SO_2 location / area
CAM5/CARMA	Jan 15, 6 h	150 Tg (~135 Tg)	25–35 km	22–14° S, 182–186° E	0.5 Tg	20–28 km	22–14° S, 182–186° E
CCSRNIES-MIROC3.2	Jan 15, instant	150 Tg (~150 Tg)	12–27.6 hPa	181.4–187.0° E, 14.0–22.3° S	–	–	–
CMAM	Feb 20, 5 days	150 Tg (~150 Tg)	~25.5 km	zonally averaged	–	–	–
EMAC MPIC	Jan 16, 12 h	136 Tg (~130 Tg)	Gaussian centered 21.5 hPa	23–19° S, 177–173° W	0.4 Tg (obs.)	23–27 km (obs.)	30° S–5° N, 90–120° W
GEOSCCM	Jan 15, 6 h	150 Tg (~150 Tg)	25–30 km	22–14° S, 182–186° E	0.5 Tg	25–30 km	22–14° S, 182–186° E
GEOS/CARMA	Jan 15, 6 h	150 Tg (~150 Tg)	25–30 km	22–14° S, 182–186° E	0.5 Tg	25–30 km	22–14° S, 182–186° E
GSFC2D	MLS H_2O profile until Mar 1	~150 Tg (~150 Tg)	–	zonally averaged	–	–	–
IFS-COMPO	Jan 15, 3 h	190 Tg (~150 Tg)	25–30 km	400×200 km area (20° S, 175° W)	0.5 Tg	25–30 km	400×200 km area (20° S, 175° W)
LMDZ6.2-LR-STRATAER	Jan 15, 1 day	150 Tg (~150 Tg)	Gaussian 27.5 km (σ = 2.5 km)	22–14° S, 182–186° E	0.5 Tg	Gaussian 27.5 km (σ = 2.5 km)	22–14° S, 182–186° E
LMDZ6.2-LR-STRATAER-REPROBUS	Jan 15, 1 day	150 Tg (~150 Tg)	Gaussian 27.5 km (σ = 2.5 km)	22–14° S, 182–186° E	0.5 Tg	Gaussian 27.5 km (σ = 2.5 km)	22–14° S, 182–186° E
MIROC-CHASER	Jan 15 (04 UTC), 6 h	186 Tg (~150 Tg)	25–30 km	22–14° S, 182–186° E	0.5 Tg	25–30 km	22–14° S, 182–186° E
UKESM1.1	Jan 15, 6 h	150 Tg	25–30 km	22–14° S, 182–186° E	0.5 Tg	25–30 km	22–14° S, 182–186° E
WACCM6/CARMA	Jan 15, 6 h	150 Tg (~150 Tg)	25–35 km	22–6° S, 182.5–202.5° E	0.5 Tg	26.5–36 km	22–6° S, 182.5–202.5° E
WACCM6/MAM	Jan 15, 6 h	150 Tg (~135 Tg)	25–35 km	22–14° S, 182–186° E	0.5 Tg	20–28 km	22–14° S, 182–186° E

lock et al. (2023) with and without Hunga Tonga. The simulated H_2O perturbation is consistent with S1.1. The SO_2 injection is derived based on the extinction from the OSIRIS observation averaged over about 10 days (Figure S1.3; Bruehl et al. 2023).

GEOSCCM

The NASA Goddard Earth Observing System Chemistry–Climate Model (GEOSCCM) is based on the GEOS Earth system model (Reinecker et al., 2008; Molod et al., 2015). For the HTHH-MOC experiments, the model was run on a cubed-sphere horizontal grid at a C90 resolution (approximately 100 km) with 72 vertical hybrid-sigma levels extending from the surface to 0.01 hPa (approximately 80 km). Dynamics are solved using the finite-volume dynamical core (Putman and Lin, 2007). Deep and shallow convection are parameterised following Grell and Freitas (2014) and Bretherton and Park (2009), respectively, while the moist physics parameterisation is from Bacmeister et al. (2006). Turbulent mixing follows the non-local scheme of Lock et al. (2000). Shortwave and longwave radiative fluxes are calculated using the Rapid Radiative Transfer Model for GCMs (RRTMG) in 30 spectral bands (Iacono et al., 2008).

Stratospheric chemistry and tropospheric chemistry are from the Global Modeling Initiative (GMI) mechanism (Duncan et al., 2007; Strahan et al., 2007; Nielsen et al., 2017), updated here to include reactions for sulfur species. The GMI mechanism in GEOSCCM has been extensively evaluated for its stratospheric ozone-related photochemistry and trans-

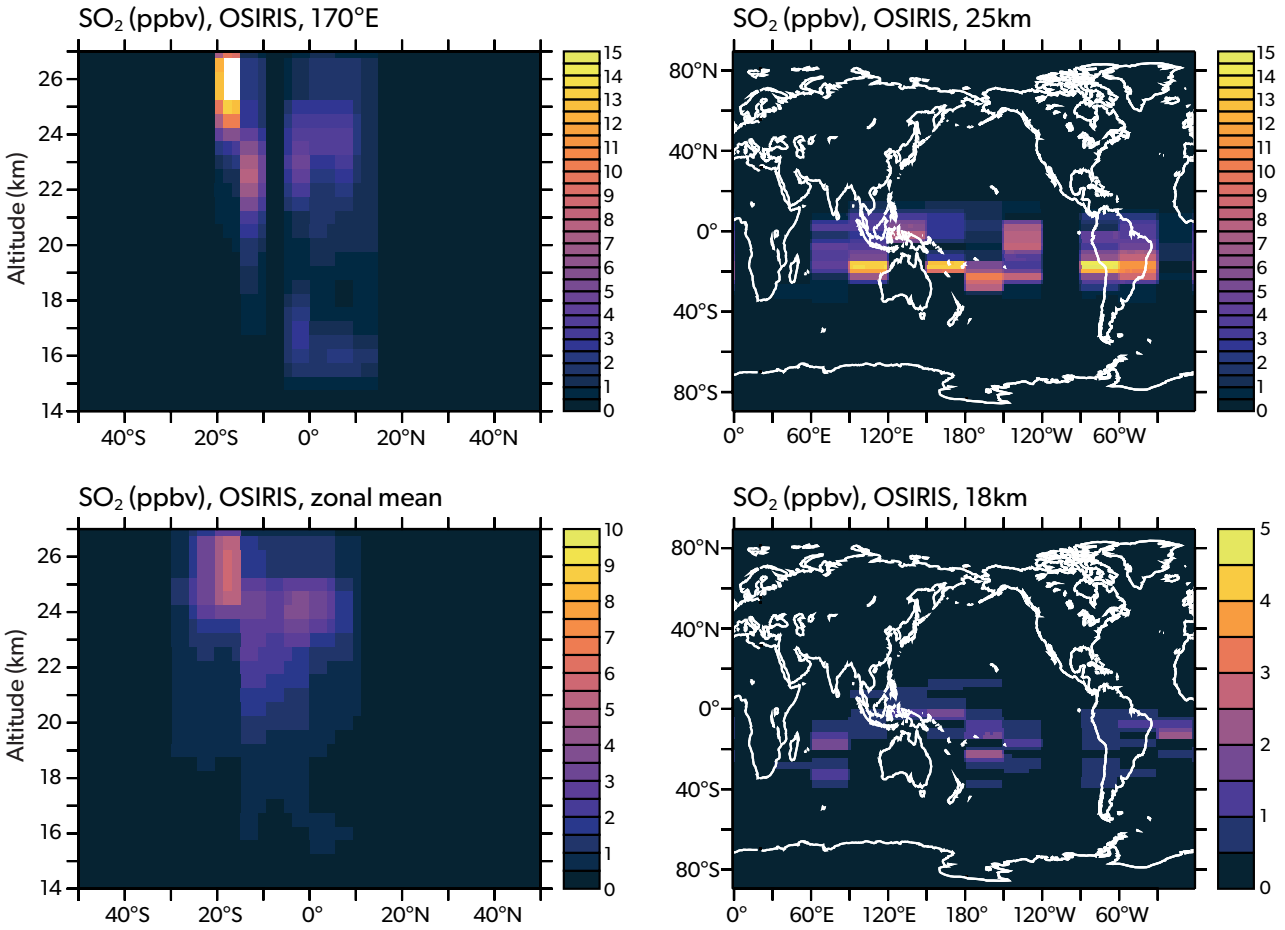

Figure S1.3: *The SO_2 injection used in the EMAC MPIC model is based on the Hunga SO_2 perturbation derived from extinction observed by OSIRIS, averaged over approximately 10 days, i.e., including several snapshots of the westward-moving plume. For conversion from extinction to volume mixing ratio, Eq. (1) of Schallock et al. (2023) is applied with $f = 3$ because of data gaps. Five-day averaged gridded OSIRIS data, averaged from 24 January at 00:00 UTC to 3 February at 00:00 UTC, were used. Note that the colour bars are not identical in each panel.*

port in various model intercomparisons, including Stratosphere-troposphere Processes and their Role in Climate (SPARC) Chemistry Climate Model Validation (CCMVal), CCMVal-2, and the CCMI (SPARC, 2010; Eyring et al., 2010; Eyring et al., 2013; Morgenstern et al., 2017).

Aerosol species are simulated by the Goddard Chemistry, Aerosol, Radiation, and Transport, second-generation (GOCART-2G) module (Collow et al., 2024), which includes a sectional approach for dust (five bins), sea salt (five bins), and nitrate (three bins) and a bulk approach for sulfate (DMS, SO_2, MSA, and SO_4^{2-}) aerosol and carbonaceous species (hydrophobic and hydrophilic modes of "white" and "brown" organics and black carbon).

For the GEOSCCM simulations performed with the GOCART-2G module we use the nominal GOCART-2G sulfate mechanism, updated here to use the online hydroxyl (OH), nitrate (NO_3), and hydrogen peroxide (H_2O_2) from the GMI mechanism instead of climatological fields provided from offline files (Collow et al., 2024). While not a full coupling to the GMI sulfur cycle it nevertheless allows the GOCART-2G sulfate mechanism to have the impact of the Hunga water vapour perturbation on the oxidants. A second "instance" of the GOCART-2G sulfate mechanism is run that is specifically for the volcanic SO_2 and resultant sulfate from the Hunga eruption. This allows us to track the eruptive volcanic aerosol separately from the nominal sulfate instance that sees mainly tropospheric sources. We assign this volcanic instance optical properties consistent with SAGE retrievals of the sulfate aerosol properties, using an effective radius of 0.4 µm.

We find that 750 Tg of H_2O is needed in the initial injection to provide a residual approximately 150 Tg of water in the stratosphere after a week. All other injection parameters follow the protocol.

The model spin-up was performed by "replaying" to the MERRA-2 meteorology (Gelaro et al., 2017), and is used throughout the Exp2a results. A MERRA-2 2012–2021 climatology of SST and sea ice fractions are used based on Reynolds et al. (2002).

GEOS/CARMA

A second configuration of the GEOSCCM, coupled to the sectional aerosol microphysics package CARMA, also simulated the eruption (GEOS/CARMA). This configuration is the same as above except for the aerosol package and its coupling to the GMI chemistry mechanism. For this version of GEOSCCM, we use the configuration of CARMA described in Case et al. (2023). This configuration uses 24 size bins, spread logarithmically in volume between 0.25 nm and 6.7 μm in radius, and simulates the nucleation, condensational growth, evaporation, coagulation, and settling of sulfate aerosols in these simulations following the mechanism of English et al. (2013).

For these simulations, CARMA is fully coupled to the GMI sulfur cycle by the production (i.e., oxidation of SO_2 and evaporation of sulfate aerosols) and loss (i.e., nucleation and condensation of sulfate aerosols) of sulfuric acid (H_2SO_4) vapour. Optical properties for the CARMA aerosols are calculated based on the interactively calculated aerosol size distribution. The same injection parameters for GEOSCCM described above are used by this configuration. This model configuration contributed to Exp2a and "replayed" to MERRA-2 meteorology as above.

GSFC2D

The NASA/Goddard Space Flight Center two-dimensional (2D) chemistry–climate model (GSFC2D) has a domain extending from the surface to approximately 92 km (0.002 hPa). The model has 76 levels, with 1 km vertical resolution from the surface to the lower mesosphere (60 km) and 2 km resolution above (60–92 km). The horizontal resolution is 4° latitude, and the model uses a 2D (latitude–altitude) finite-volume dynamical core (Lin and Rood, 1996) for advective transport. The model has detailed stratospheric chemistry and reduced tropospheric chemistry, with a diurnal cycle computed for all constituents each day (Fleming et al., 2024). The model uses prescribed zonal mean surface temperature as a function of latitude and season based on a multi-year average of MERRA-2 data (Gelaro et al., 2017). Zonal mean latent heating, tropospheric water vapour, and cloud radiative properties as a function of latitude, altitude, and season are also prescribed (Fleming et al., 2020).

For the free-running simulations, the model planetary wave parameterisation follows Bacmeister et al. (1995) and Fleming et al. (2024) and uses lower boundary conditions (750 hPa, approximately 2 km) of geopotential height amplitude and phase for zonal wave numbers 1–4. These are derived as a function of latitude and season using (1) a 30-year average (1991–2020) of MERRA-2 data for the standard yearly repeating climatological-dynamics simulations ("Clim-NoQBO") and (2) individual years of MERRA-2 data (1980–2020), randomly rearranged in time to generate interannual variations in stratospheric dynamics ("ensemble1", "ensemble2", … "ensemble10"). For the inter-annually varying dynamics simulations, the model includes an internally generated QBO (Fleming et al., 2024).

For experiments that include the Hunga volcanic aerosols, the simulations go through the end of 2023, using prescribed aerosol properties for 2022–2023 both from the GloSSAC dataset and from the OMPS-LP data (Taha et al., 2021; Taha et al., 2022). For experiments that include the Hunga H_2O injection, Aura/MLS observations are used to derive a daily zonal mean Hunga water vapour anomaly in latitude–altitude, which is added to the baseline H_2O (no volcano) through the end of February 2022. This combined water vapor field is then fully model computed starting 1 March 2022 through the end of 2031.

For Exp2b, the model zonal mean temperature and transport fields are computed from the MERRA-2 reanalysis data. These are input into the model and used as prescribed fields (no nudging is done).

IFS-COMPO

The Copernicus Atmosphere Monitoring Service (CAMS) provides daily global analysis and 5-day forecasts of atmospheric composition (aerosols, trace gases, and greenhouse gases, GHGs) (Peuch et al., 2022). CAMS is coordinated by the European Centre for Medium Range Weather Forecasts (ECMWF) and uses, for its global component, the Integrated Forecasting System (IFS), with extensions to represent aerosols, trace, and GHGs, being called "IFS-COMPO" (also previously known as "C-IFS", Flemming et al. 2015).

IFS-COMPO is composed of IFS(AER) for aerosols, as described in Rémy et al. (2022), while the atmospheric chemistry is based on the chemistry module as described in Williams et al. (2022) for the tropo-

sphere (IFS-CB05) and Huijnen et al. (2016) for the stratosphere (IFS-CBA). The stratospheric chemistry module of IFS-COMPO is derived from the Belgian Assimilation System for Chemical ObsErvations (BASCOE; Errera et al. 2019). IFS-COMPO stratospheric chemistry is used since the operational implementation of cycle 48R1 on 27 June 2023 (Eskes et al., 2024).

The aerosol component of IFS-COMPO is a bulk aerosol scheme for all species except sea salt aerosol and desert dust, for which a sectional approach is preferred, with three bins for each of these two species. Since the implementation of operational cycle 48R1 in June 2023, the prognostic species are sea salt, desert dust, organic matter (OM), black carbon (BC), sulfate, nitrate, ammonium, and secondary organic aerosols (SOAs).

For Exp2a, cycle 49R1 IFS-COMPO has been used, which will become operational for CAMS production in November 2024, at a resolution of TL511 (approximately 40 km) over 137 model levels from surface to 0.01 hPa. Cycle 49R1 IFS-COMPO integrates a number of updates of tropospheric and stratospheric aerosols and chemistry. The most relevant aspect for this work concerns the representation of stratospheric aerosols, which has been revisited with the implementation of a coupling to the stratospheric chemistry through a simplified stratospheric sulfur cycle including nucleation/condensation and evaporation processes, as shown in Figure 1.4. Direct injection of water vapour into the stratosphere is expected to enhance the nucleation and condensation of sulfate through the reaction with SO_3 and production of gas-phase H2SO4. The volcanic injection takes place between 03:00 and 06:00 UTC on 15 January 2022, with a uniform vertical distribution between 25 and 30 km of altitude, over a rectangular region of 400 km (latitude) × 200 km (longitude) centred on the coordinates of the Hunga volcano. The injected quantities are 0.5 Tg SO2 and 190 Tg H_2O.

LMDZ6.2-LR-STRATAER and LMDZ6.2-LR-STRATAER-REPROBUS

The Institut Pierre-Simon Laplace Climate Modelling Centre (IPSL CMC; `https://cmc.ipsl.fr/`, last access: 12 August 2025) has set up a new version of its climate model in the runup to CMIP6. Further description of the IPSL-CM6A-LR climate model can be found in Boucher et al. (2020) and in Lurton et al. (2020). New development of the model is now ongoing to prepare the IPSLCM7 version.

The IPSLCM7 climate model is using the general circulation model named LMDZ (Laboratoire de Météorologie Dynamique-Zoom; Hourdin et al. 2006). The LMDZ version used for this study is based on a regular horizontal grid with 144 points regularly spaced in longitude and 142 in latitude, corresponding to a resolution of 2.5° × 1.3°. The model has 79 vertical layers and extends up to 80 km, which makes it a "high-top" model. The model shows a self-generated quasi-biennial oscillation (QBO), whose period has been tuned to the observed one for the present-day climate (Boucher et al., 2020).

The aerosol is interactively simulated in the STRATAER module using a sectional scheme with 36 size bins. STRATAER is an improved version of the Sectional Stratospheric Sulfate Aerosol (S3A) module (Kleinschmitt et al., 2017). It now takes into account the photolytic conversion of H_2SO_4 into SO_2 in the upper stratosphere (Mills et al., 2005). The size-dependent composition of H_2SO_4/H_2O aerosols is now computed iteratively to ensure that the surface tension, density, and composition are consistent in the calculation of the Kelvin effect. The surface tension, density, H_2SO_4 vapour pressure, and nucleation rates are calculated based on Vehkamäki et al. (2002). The version of the LMDZ6.2-LR-STRATAER atmospheric model used in the HTHH Impact project accounts for the stratospheric H_2O source from methane oxidation. The chemistry is simulated using the REPROBUS (REactive Processes Ruling the Ozone BUdget in the Stratosphere) chemistry module that includes 55 chemical species and a comprehensive description of the stratospheric chemistry (Marchand et al., 2012; Lefèvre et al., 1994; Lefèvre et al., 1998).

For Exp2a, the H_2O and SO_2 are injected at 27.5 km altitude using a Gaussian distribution and standard deviation of 2.5 km. The injection latitude ranges from 22 to 14°S, and longitude ranges from 182 to 186°E. The injections of H_2O and SO_2 are 150 and 0.5 Tg, respectively. The SSTs are taken from the IPSL climate-coupled simulation run under the CMIP6 Tier 1 SSP2-4.5 scenario (O'Neill et al., 2016).

MIROC-CHASER

The Model for Interdisciplinary Research On Climate – CHemical Atmospheric general circulation model for Study of atmospheric Environment and Radiative forcing (MIROC-CHASER) version 6 (Sekiya et al., 2016) is a chemistry climate model, with a top at around 0.004 hPa. The present version of MIROC-CHASER is built on MIROC6 (Tatebe et al., 2019) and has a spectral horizontal resolution of T85 (1.4° lat-

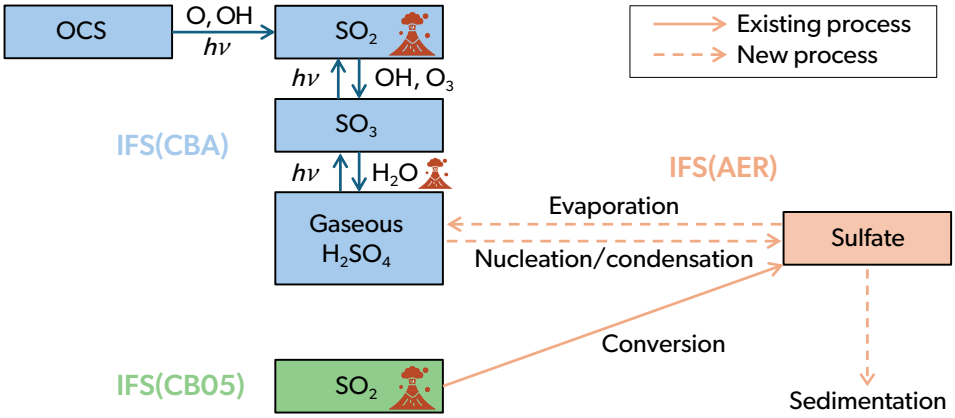

Figure S1.4: *Architecture of the stratospheric extension of IFS(AER) and its coupling with IFS(CBA) and IFS(CB05), with existing and new processes implemented in cycle 49R1 of IFS-COMPO. hν represents photolysis, and the volcano symbols represent direct injections by volcanic eruptions. Sedimentation is indicated as a new process because it has been revisited.*

itude × 1.4° longitude). The model has 81 vertical levels, with a vertical resolution 0.7 km in the lower stratosphere, ~1.2 km in the upper stratosphere, and ~3 km in the lower mesosphere. In the free-running simulations, the model generates the QBO internally. The ensemble members have different initial conditions (1 January 2022), which are generated using slightly different nudging relaxation time during the spin-up. The aerosols are interactively simulated using a three-mode modal aerosol module (Sekiya et al., 2016). The chemistry uses comprehensive troposphere–stratosphere chemistry (Watanabe et al., 2011). The volcanic emission from continuously degassing volcanoes uses the emission inventory of Fioletov et al. (2022). For the explosive volcanic eruptions during the spin-up time, explosive volcanic emissions follow Carn et al. (2022).

For Exp1 fixed-SST simulations, the model uses the observed SST from 10-year climatological mean from 2012 to 2021 using the monthly-1deg CMIP6 AMIP SST (Gates et al., 1999).

For Exp2a, the atmospheric temperature and winds are nudged to MERRA-2 reanalysis with a 12 h relaxation using 3 h meteorology. The observed SST uses the NOAA 1/4° Daily Optimum Interpolation Sea Surface Temperature (OISST) from 2022 to 2023 (Huang et al., 2020).

The initial volcanic injection altitude and area are not tuned but follow the experimental protocol. For Exp1 and Exp2a, the H2O and SO2 are injected at 25 to 30 km altitude. The injection latitude ranges from 22 to 14°S, and longitude ranges from 182 to 186°E. The initial injection of H_2O is 186 Tg, with ~150 Tg left after the first week following the eruption. The large initial H_2O injection is necessary to keep 150 Tg in the stratosphere as requested by the experimental protocol because a large amount of ice clouds generates and falls to the troposphere soon after the eruption.

UKESM1.1

The United Kingdom Earth System Model (UKESM, Sellar et al. 2019; Sellar et al. 2020) is the successor to the HadGEM2-ES model (Collins et al., 2011), jointly developed by the UK Met Office and the Natural Environment Research Council (NERC) to deliver simulations to the Coupled Model Intercomparison Project Phase 6 (CMIP6; Eyring et al. 2016). For HTHH-MOC, we run the updated UKESM1.1 system (Mulcahy et al., 2023), which consists of the physical climate model HadGEM3-GC3.1 (Kuhlbrodt et al., 2018; Williams et al., 2018) and has improved tropospheric aerosol processes and aerosol radiative forcings (Mulcahy et al., 2018; Mulcahy et al., 2020). The GC3.1 system comprises the GA7.1 global atmosphere model configuration (Walters et al., 2019), which uses the ENDGAME dynamics system (Wood et al., 2014), at a resolution of 1.875° longitude by 1.25° latitude, with 85 levels extending to 85 km. Specifically the simulations apply the UKESM1.1-AMIP academic community release job (at v12.1 of the Unified Model), as supported by the UK National Centre for Atmospheric Science.

The interactive atmospheric chemistry module UKCA (UK Chemistry and Aerosols) has a number of chemistry configurations, with UKESM1.0 for CMIP6 applying the combined stratosphere and troposphere chemistry (CheST) option (Archibald et al., 2020), essentially a combination of the stratosphere chemistry (Morgenstern et al., 2009) and tropospheric chem-

istry (O'Connor et al., 2014) UKCA schemes. The UKCA aerosol scheme is the GLOMAP-mode aerosol microphysics module (Mann et al., 2010; Mann et al., 2012; Bellouin et al., 2013), with UKESM1.0 including the initial set of adaptations to GLOMAP for simulating stratospheric aerosol Dhomse et al. (2014). For all UKESM1.0 integrations for CMIP6, the system was applied with evaporation of sulfate aerosol de-activated, stratospheric aerosol properties enacted from the CMIP6-prescribed zonal mean dataset (Luo, 2017; Jörimann, 2025), but for the integrations here we have applied the system for interactive aerosol across the troposphere and stratosphere, enacting a Hunga emission of volcanic SO2 following the 0.5 Tg at 25–30 km Tonga-MIP protocols (see Table S1.6).

For the improved UKESM1.1 version applied here, the other most relevant development, compared to UKESM1.0 used for CMIP6, is the interactive atmospheric chemistry module UKCA (UK Chemistry and Aerosols), which has the updates to heterogeneous chemistry added by Dennison et al. (2019), to represent reactions occurring on the surfaces of polar stratospheric clouds and sulfate aerosol more realistically, with modified uptake coefficients of the five existing reactions and the addition of a further eight reactions involving bromine species. For these simulations, for the first time we have added the equilibrium liquid PSC scheme of Carslaw et al. (1995) to UKESM; this scheme is an interim implementation here coupling the five existing heterogeneous reactions of chlorine activation here then occurring on solid and now also liquid ternary-aerosol PSCs.

For Exp2, UKESM1.1 is run in a specified dynamics configuration (Telford et al., 2008; Telford et al., 2009), the atmospheric temperature and winds nudged to ERA5 every 6 h, the Newton relaxation applied for levels 12 to 80 of 85 (between 1 and 60 km). Sea-surface temperatures and sea ice are prescribed from the Reynolds v2.1 datasets, during both the 2017 to 2022 spin-up period and the 2-year Exp2 period to December 2023. Monthly varying anthropogenic atmospheric chemistry and aerosol emissions were set following the CMIP6 SSP2-4.5 datasets.

WACCM6/MAM4

The Whole Atmosphere Community Climate Model version 6 (WACCM6; Gettelman et al. 2019) is the high-top version of the atmospheric component of the Community Earth System Model, version 2 (CESM2), with a top at around 140 km. WACCM6 has a horizontal resolution of 0.9° latitude × 1.25° longitude, utilising the finite-volume dynamical core (Lin and Rood, 1996). The model has 70 vertical levels, with a vertical resolution of ~1 km in the lower stratosphere, ~1.75 km in the upper stratosphere, and ~3.5 km in the upper mesosphere and lower thermosphere (Garcia et al., 2017). In the free-running simulations, the model generates QBO internally (Mills et al., 2017; Gettelman et al., 2019). The ensemble members differ in the last date of nudging (from 27 January to 5 February 2022). The aerosol is interactively simulated using a four-mode modal aerosol module (MAM4; Liu et al. 2012; Liu et al. 2016; Mills et al. 2016), in which we used the Vehkamäki nucleation scheme Vehkamäki et al. (2002). The chemistry uses comprehensive troposphere–stratosphere–mesosphere–lower thermosphere (TSMLT) chemistry (Gettelman et al., 2019). The volcanic emissions from continuously degassing volcanoes use the emission inventory of Andres and Kasgnoc (1998). For the explosive volcanic eruptions during the spin-up time, explosive volcanic emissions follow Mills et al. (2016) and Neely III and Schmidt (2016), with updates until 2022.

For Exp1_CoupledOcean simulations, the ocean and sea ice are initialised on 3 January 2022 with output from a standalone ocean model forced by atmospheric state fields and fluxes from the Japanese 55-year Reanalysis (Tsujino et al., 2018). To accurately simulate the early plume structure and evolution, the winds and temperatures in WACCM are nudged toward the Analysis for Research and Applications, MERRA-2 meteorological data (Gelaro et al., 2017) throughout January 2022. After 1 February 2022, the model is free-running to capture fully coupled variability. For the fixed-SST simulation, the model uses the 10-year climatology SST from 2012 to 2021. The SST data are OISSTv2, which is a NOAA High-resolution (0.25 × 0.25) Blended Analysis of Daily SST and Ice (Banzon et al., 2022).

For Exp2, the atmospheric temperature and winds are nudged to MERRA-2 reanalysis with a 12 h relaxation using 3 h meteorology (Davis et al., 2022). The observed SST uses the 10-year climatological mean from 2012 to 2021.

The initial volcanic injection altitude and area are the same as described in Section S1.4 for CAM5/CARMA.

WACCM6/CARMA

WACCM6/CARMA only performed Exp2 and used a configuration similar to WACCM6/MAM4 with

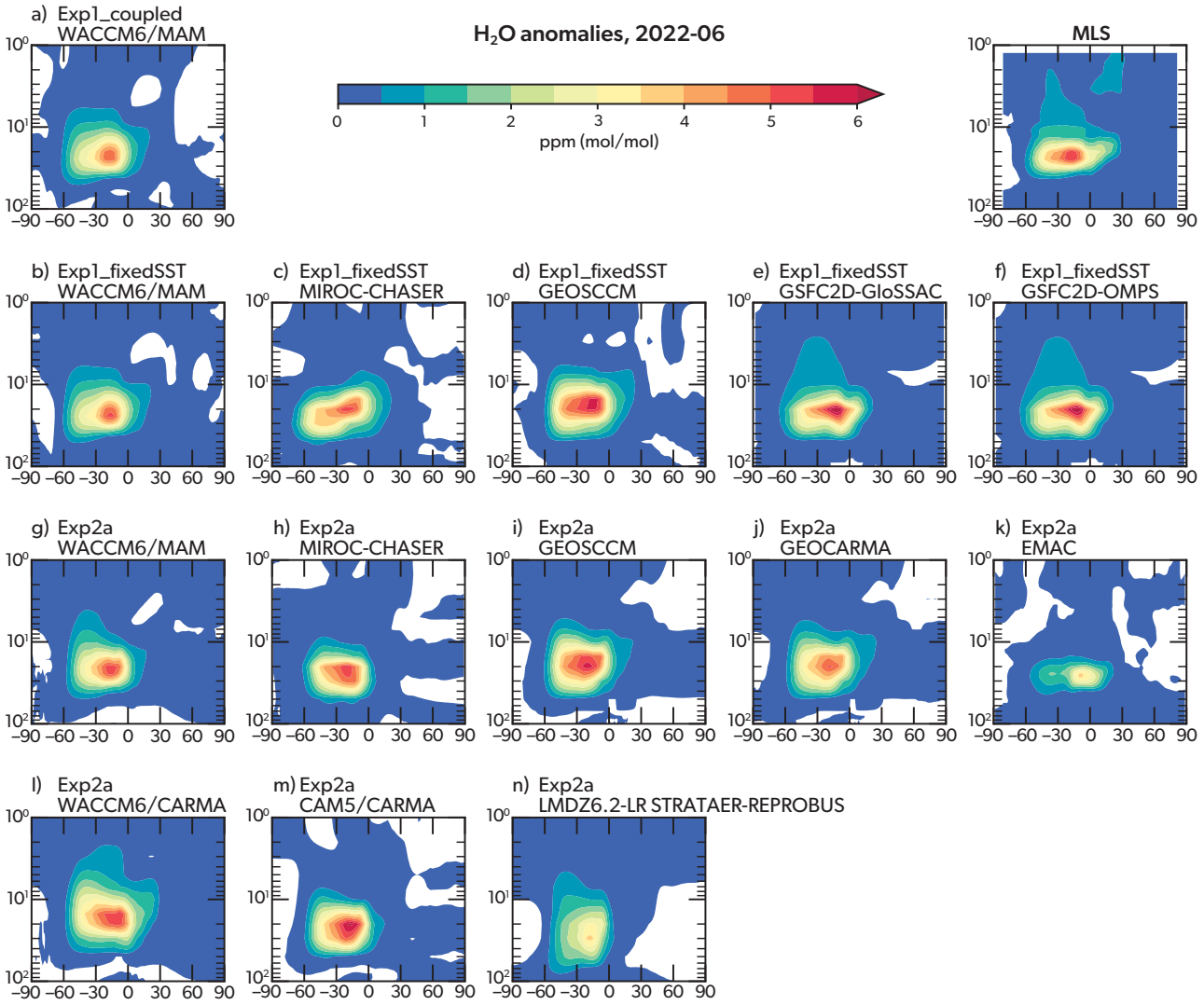

Figure S1.5: *The zonal average H_2O anomaly in June 2022 from MLS, Exp1_fixedSST, Exp1_CoupledOcean, and Exp2a. The simulated anomaly is using the H_2O + SO_2 run minus the control run. And the MLS uses the 2022 data minus the climatology.*

the same horizontal and vertical resolution, SSTs, and meteorological nudging. Differences compared to WACCM6/MAM4 are the chemistry and aerosol configuration used. WACCM6/CARMA used the middle atmosphere chemistry with limited chemistry in the troposphere and comprehensive chemistry in the stratosphere, mesosphere, and lower thermosphere (Davis et al., 2022). Furthermore, we use the Community Aerosol and Radiation Model for Atmospheres (CARMA, Tilmes et al. 2023), based on Yu et al. (2015) with some updates) as the aerosol module, in which we used the Vehkamäki nucleation scheme (Vehkamäki et al., 2002). CARMA defines 20 mass bins and tracks the dry mass of the particles and assumes particle water is in equilibrium with the environmental water vapour. The approximate radius ranges from 0.2 nm to 1.3 μm in radius for the pure sulfate group that sulfate homogeneous nucleation occurs in and ranges from 0.05 to 8.7 μm in the mixed group that tracks all major tropospheric aerosol types (i.e., black carbon, organic carbon, sea salt, dust, sulfate).

The initial volcanic injection altitude and area are determined by validating the water and aerosol transportation in the first 6 months against MLS and OMPS observations. In these simulations, the H_2O is injected to 25 to 35 km altitude following Zhu et al. (2022), while the SO_2 is injected 82% of the total mass to 26.5–28 km and 18% to 28–36 km altitude. The injection latitude ranges from 22 to 6°S, and longitude ranges from 182.5 to 202.5°E.

S1.5 Preliminary results

The models' performances will be evaluated focusing on the following aspects: the stratospheric aerosol optical depth will be compared with GloSSAC and other satellite instruments individually such as OMPS-LP, SAGEIII-ISS, and OSIRIS; the aerosol effective radius will be compared with balloon observations (Asher et al., 2023), SAGEIII-ISS-retrieved size distribution, and AeroNet-retrieved particle radius; the water vapour lifetime, ozone, and its related chemicals (such as HCl, HNO_3, and ClO) will be compared with MLS observations; and the temperature anomaly will be compared with the MLS detrended temperature field (Randel et al., 2024). All the evaluations will be conducted before looking into the climate impact of this eruption, such as radiative impact and tropospheric responses. This work will be described in a follow-up paper.

As the time of writing, we are still completing the model output inspection and validation phase. So, we can only provide preliminary results from some models. Figure S1.5 shows the preliminary results from Exp1 and Exp2 in June 2022 compared with the MLS v5 water vapour anomaly. The model results shown here generally agree with the MLS anomaly regarding the vertical (10–50 hPa) and horizontal distribution (60°S to 20°N) and the anomaly peaking at ~6 ppmv for most of the models. This consistency of water vapour anomaly 6 months after the eruption helps us have confidence in these models for the analysis of climate and chemistry impacts and will be evaluated in detail in the follow up studies.

S1.6 Summary

A multi-model observation comparison project is designed to evaluate the impact of the 2022 Hunga eruption. Two experiments are designed to cover various research interests for this eruption, including sulfate and water plume dispersion and transport, dynamical and chemical responses in the stratosphere, and climate impact. The project will not only benefit the Hunga Impact assessment but also benchmark the model performance in simulating stratospheric explosive volcanic eruption events and stratospheric water vapour injections. These events have a potentially large impact on the Earth system, especially on the stratospheric ozone layer and radiative balance.

Code/Data availability

The data used to produce the results used in this paper is archived on Zenodo:

`https://doi.org/10.5281/zenodo.14962954` (Wang, 2025).

`https://doi.org/10.5281/zenodo.14963276` (Quaglia et al., 2023; Zhuo et al., 2025).

`https://doi.org/10.5281/zenodo.14961868` (Jörimann, 2025).

`https://doi.org/10.5281/zenodo.14962925` (Brühl, 2025).

References

Akiyoshi, H., M. Kadowaki, Y. Yamashita and T. Nagatomo (2023). 'Dependence of column ozone on future ODSs and GHGs in the variability of 500-ensemble members'. *Sci. Rep.*, 13, 320. DOI: 10.1038/s41598-023-27635-y.

Akiyoshi, H., T. Nakamura, T. Miyasaka, M. Shiotani and M. Suzuki (2016). 'A nudged chemistry-climate model simulation of chemical constituent distribution at northern high-latitude stratosphere observed by SMILES and MLS during the 2009/2010 stratospheric sudden warming'. *J. Geophys. Res.*, 121, pp. 1361–1380. DOI: 10.1002/2015JD023334.

Andres, R. J. and A. D. Kasgnoc (1998). 'A time-averaged inventory of subaerial volcanic sulfur emissions'. *J. Geophys. Res.*, 103, pp. 25251–25261. DOI: 10.1029/98JD02091.

Archibald, A. T., F. M. O'Connor, N. L. Abraham, S. Archer-Nicholls, M. P. Chipperfield, M. Dalvi, G. A. Folberth, F. Dennison, S. S. Dhomse, P. T. Griffiths et al. (2020). 'Description and evaluation of the UKCA stratosphere–troposphere chemistry scheme (StratTrop vn 1.0) implemented in UKESM1'. *Geosci. Model Dev.*, 13, pp. 1223–1266. DOI: 10.5194/gmd-13-1223-2020.

Asher, E., M. Todt, K. Rosenlof, T. Thornberry, R.-S. Gao, G. Taha, P. Walter, S. Alvarez, J. Flynn, S. M. Davis et al. (2023). 'Unexpectedly rapid aerosol formation in the Hunga Tonga plume'. *Proc. Natl. Acad. Sci.*, 120, e2219547120. DOI: 10.1073/pnas.2219547120.

Bacmeister, J. T., M. R. Schoeberl, M. E. Summers, J. E. Rosenfield and X. Zhu (1995). 'Descent of long-lived trace gases in the winter polar vortex'. *J. Geophys. Res.*, 100, pp. 11669–11684. DOI: 10.1029/94JD02958.

Bacmeister, J. T., M. J. Suarez and F. R. Robertson (2006). 'Rain reevaporation, boundary layer–convection interactions, and Pacific rainfall patterns in an AGCM'. *J. Atmos. Sci.*, 63, pp. 3383–3403. DOI: 10.1175/jas3791.1.

Banzon, V., R. Reynolds and N. C. for Atmospheric Research Staff (Eds.) (2022). *The Climate Data Guide: SST data: NOAA High-resolution (0.25×0.25) Blended Analysis of Daily SST and Ice, OISSTv2.* https://climatedataguide.ucar.edu/climate-data/sst-data-noaa-high-resolution-025x025-blended-analysis-daily-sst-and-ice-oisstv2. Last access: 4 February 2025.

Bellouin, N., G. W. Mann, M. T. Woodhouse, C. Johnson, K. S. Carslaw and M. Dalvi (2013). 'Impact of the modal aerosol scheme GLOMAP-mode on aerosol forcing in the Hadley Centre Global Environmental Model'. *Atmos. Chem. Phys.*, 13, pp. 3027–3044. DOI: 10.5194/acp-13-3027-2013.

Bernath, P. F., C. T. McElroy, M. C. Abrams, C. D. Boone, M. Butler, C. Camy-Peyret, M. Carleer, C. Clerbaux, P.-F. Coheur, R. Colin et al. (2005). 'Atmospheric Chemistry Experiment (ACE): Mission overview'. *Geophys. Res. Lett.*, 32, L15S01. DOI: 10.1029/2005GL022386.

Boucher, O., J. Servonnat, A. L. Albright, O. Aumont, Y. Balkanski, V. Bastrikov, S. Bekki, R. Bonnet, S. Bony, L. Bopp et al. (2020). 'Presentation and evaluation of the IPSL-CM6A-LR climate model'. *J. Adv. Model. Earth Syst.*, 12, e2019MS002010. DOI: 10.1029/2019MS002010.

Bretherton, C. S. and S. Park (2009). 'A new moist turbulence parameterization in the Community Atmosphere Model'. *J. Climate*, 22, pp. 3422–3448. DOI: 10.1175/2008jcli2556.1.

Brodowsky, C., T. Sukhodolov, A. Feinberg, M. Höpfner, T. Peter, A. Stenke and E. Rozanov (2021). 'Modeling the sulfate aerosol evolution after recent moderate volcanic activity, 2008–2012'. *J. Geophys. Res.*, 126, e2021JD035472. DOI: 10.1029/2021JD035472.

Bruehl, C., J. Lelieveld, J. Schallock and L. A. Rieger (2023). 'Chemistry Climate Model Studies on the Effect of the Hunga Tonga Eruption on Stratospheric Ozone in Mid and High Latitudes in 2022'. *AGU Fall Meeting Abstracts*. Vol. 2023. 2235. https://ui.adsabs.harvard.edu/abs/2023AGUFM.A21B2235B, A21B–2235.

Brühl, C. (2025). *SO_2 emission for EMAC MPIC model.* Zenodo. DOI: 10.5281/zenodo.14962925.

Carn, S., V. Fioletov, C. McLinden, C. Li and N. A. Krotkov (2017). 'A decade of global volcanic SO_2 emissions measured from space'. *Sci. Rep.*, 7, 44095. DOI: 10.1038/srep44095.

Carn, S. A., L. Clarisse and A. J. Prata (2016). 'Multi-decadal satellite measurements of global volcanic degassing'. *J. Volcanol. Geotherm. Res.*, 311, pp. 99–134. DOI: 10.1016/j.jvolgeores.2016.01.002.

Carn, S. A., N. A. Krotkov, B. L. Fisher and C. Li (2022). 'Out of the blue: volcanic SO_2 emissions during the 2021-2022 Hunga Tonga-Hunga Ha'apai eruptions'. *Front. Earth Sci.*, 13. DOI: 10.3389/feart.2022.976962.

Carslaw, K. S., B. Luo and T. Peter (1995). 'An analytic expression for the composition of aqueous HNO_3–H_2SO_4 stratospheric aerosols including gas phase

removal of HNO_3'. *Geophys. Res. Lett.*, 22, pp. 1877–1880. DOI: 10.1029/95GL01668.

Case, P., P. R. Colarco, O. B. Toon, V. Aquila and C. A. Keller (2023). 'Interactive stratospheric aerosol microphysics-chemistry simulations of the 1991 Pinatubo volcanic aerosols with newly coupled sectional aerosol and stratosphere-troposphere chemistry modules in the NASA GEOS Chemistry-Climate Model (CCM)'. *J. Adv. Model. Earth Syst.*, 15, e2022MS003147. DOI: 10.1029/2022MS003147.

Clyne, M., O. B. Toon, T. Sukhodolov, G. W. Mann, S. Dhomse, S. Tilmes, Y. Zhu, P. R. Colarco, K. Tsigaridis, T. Nagashima et al. (2024). 'Tonga-MIP: The Hunga Tonga-Hunga Ha'apai Volcano Model Intercomparison Project'. In M. Clyne (Ed.), *Modeling the role of volcanoes in the climate system* (Publication No. 31487034), https://www.proquest.com/dissertations-theses/modeling-role-volcanoes-climate-system/docview/3100397790/se-2. PhD thesis. University of Colorado at Boulder.

Collins, W. J., N. Bellouin, M. Doutriaux-Boucher, N. Gedney, P. Halloran, T. Hinton, J. Hughes, C. D. Jones, M. Joshi, S. Liddicoat et al. (2011). 'Development and evaluation of an Earth-System model – HadGEM2'. *Geosci. Model Dev.*, 4, pp. 1051–1075. DOI: 10.5194/gmd-4-1051-2011.

Collow, A. B., P. R. Colarco, A. M. da Silva, V. Buchard, H. Bian, M. Chin, S. Das, R. Govindaraju, D. Kim and V. Aquila (2024). 'Benchmarking GOCART-2G in the Goddard Earth Observing System (GEOS)'. *Geosci. Model Dev.*, 17, pp. 1443–1468. DOI: 10.5194/gmd-17-1443-2024.

Davis, N. A., P. Callaghan, I. R. Simpson and S. Tilmes (2022). 'Specified dynamics scheme impacts on wave-mean flow dynamics, convection, and tracer transport in CESM2 (WACCM6)'. *Atmos. Chem. Phys.*, 22, pp. 197–214. DOI: 10.5194/acp-22-197-2022.

Dennison, F., J. Keeble, O. Morgenstern, G. Zeng, N. L. Abraham and X. Yang (2019). 'Improvements to stratospheric chemistry scheme in the UM-UKCA (v10.7) model: solar cycle and heterogeneous reactions'. *Geosci. Model Dev.*, 12, pp. 1227–1239. DOI: 10.5194/gmd-12-1227-2019.

Dhomse, S. S., K. M. Emmerson, G. W. Mann, N. Bellouin, K. S. Carslaw, M. P. Chipperfield, R. Hommel, N. L. Abraham, P. Telford, P. Braesicke et al. (2014). 'Aerosol microphysics simulations of the Mt. Pinatubo eruption with the UM-UKCA composition-climate model'. *Atmos. Chem. Phys.*, 14, pp. 11221–11246. DOI: 10.5194/acp-14-11221-2014.

Dhomse, S. S., G. W. Mann, J. C. Antuña Marrero, S. E. Shallcross, M. P. Chipperfield, K. S. Carslaw, L. Marshall, N. L. Abraham and C. E. Johnson (2020). 'Evaluating the simulated radiative forcings, aerosol properties, and stratospheric warmings from the 1963 Mt Agung, 1982 El Chichón, and 1991 Mt Pinatubo volcanic aerosol clouds'. *Atmos. Chem. Phys.*, 20, pp. 13627–13654. DOI: 10.5194/acp-20-13627-2020.

Duncan, B. N., J. A. Logan, I. Bey, I. A. Megretskaia, R. M. Yantosca, P. C. Novelli, N. B. Jones and C. P. Rinsland (2007). 'Global budget of CO, 1988–1997: Source estimates and validation with a global model'. *J. Geophys. Res.*, 112, D22301. DOI: 10.1029/2007JD008459.

Emmons, L. K., S. Walters, P. G. Hess, J.-F. Lamarque, G. G. Pfister, D. Fillmore, C. Granier, A. Guenther, D. Kinnison, T. Laepple et al. (2010). 'Description and evaluation of the Model for Ozone and Related chemical Tracers, version 4 (MOZART-4)'. *Geosci. Model Dev.*, 3, pp. 43–67. DOI: 10.5194/gmd-3-43-2010.

English, J. M., O. B. Toon, M. J. Mills and F. Yu (2011). 'Microphysical simulations of new particle formation in the upper troposphere and lower stratosphere'. *Atmos. Chem. Phys.*, 11, pp. 9303–9322. DOI: 10.5194/acp-11-9303-2011.

English, J. M., O. B. Toon and M. J. Mills (2013). 'Microphysical simulations of large volcanic eruptions: Pinatubo and Toba'. *J. Geophys. Res.*, 118, pp. 1880–1895. DOI: 10.1002/jgrd.50196.

Errera, Q., S. Chabrillat, Y. Christophe, J. Debosscher, D. Hubert, W. Lahoz, M. L. Santee, M. Shiotani, S. Skachko, T. von Clarmann et al. (2019). 'Technical note: Reanalysis of Aura MLS chemical observations'. *Atmos. Chem. Phys.*, 19, pp. 13647–13679. DOI: 10.5194/acp-19-13647-2019.

Eskes, H., A. Tsikerdekis, M. Ades, M. Alexe, A. C. Benedictow, Y. Bennouna, L. Blake, I. Bouarar, S. Chabrillat, R. Engelen et al. (2024). 'Technical note: Evaluation of the Copernicus Atmosphere Monitoring Service Cy48R1 upgrade of June 2023'. *Atmos. Chem. Phys.*, 24, pp. 9475–9514. DOI: 10.5194/acp-24-9475-2024.

Eyring, V., S. Bony, G. A. Meehl, C. A. Senior, B. Stevens, R. J. Stouffer and K. E. Taylor (2016). 'Overview of the Coupled Model Intercomparison Project Phase 6 (CMIP6) experimental design and organ-

ization'. *Geosci. Model Dev.*, 9, pp. 1937–1958. DOI: 10.5194/gmd-9-1937-2016.

Eyring, V., I. Cionni, G. E. Bodeker, A. J. Charlton-Perez, D. E. Kinnison, J. F. Scinocca, D. W. Waugh, H. Akiyoshi, S. Bekki, M. P. Chipperfield et al. (2010). 'Multi-model assessment of stratospheric ozone return dates and ozone recovery in CCMVal-2 models'. *Atmos. Chem. Phys.*, 10, pp. 9451–9472. DOI: 10.5194/acp-10-9451-2010.

Eyring, V., J.-F. Lamarque, P. Hess, F. Arfeuille, K. Bowman, M. P. Chipperfield, B. Duncan, A. Fiore, A. Gettelman, M. A. Giorgetta et al. (2013). *Overview of the IGAC/SPARC Chemistry-Climate Model Initiative (CCMI) Community Simulations in Support of Upcoming Ozone and Climate Assessments*. http://www.aparc-climate.org/wp-content/uploads/2017/12/SPARCnewsletter_No40_Jan2013_web.pdf. SPARC Newsletter No. 40, Last access: 21 August 2025.

Fioletov, V., C. A. McLinden, D. Griffin, I. Abboud, N. Krotkov, P. J. T. Leonard, C. Li, J. Joiner, N. Theys and S. Carn (2022). *Multi-Satellite Air Quality Sulfur Dioxide (SO_2) Database Long-Term L4 Global V2*. Ed. by P. Leonard. Greenbelt, MD, USA: Goddard Earth Science Data and Information Services Center (GES DISC). DOI: 10.5067/MEASURES/SO2/DATA406.

Fleming, E. L., P. A. Newman, Q. Liang and J. S. Daniel (2020). 'The Impact of Continuing CFC-11 Emissions on Stratospheric Ozone'. *J. Geophys. Res.*, 125, e2019JD031849. DOI: 10.1029/2019jd031849.

Fleming, E. L., P. A. Newman, Q. Liang and L. D. Oman (2024). 'Stratospheric Temperature and Ozone Impacts of the Hunga Tonga-Hunga Ha'apai Water Vapor Injection'. *J. Geophys. Res.*, 129, e2023JD039298. DOI: 10.1029/2023jd039298.

Flemming, J., V. Huijnen, J. Arteta, P. Bechtold, A. Beljaars, A.-M. Blechschmidt, M. Diamantakis, R. J. Engelen, A. Gaudel, A. Inness et al. (2015). 'Tropospheric chemistry in the Integrated Forecasting System of ECMWF'. *Geosci. Model Dev.*, 8, pp. 975–1003. DOI: 10.5194/gmd-8-975-2015.

Fomichev, V. I., C. Fu, J. de Grandpré, S. R. Beagley, V. P. Ogibalov and J. C. McConnell (2004). 'Model thermal response to minor radiative energy sources and sinks in the middle atmosphere'. *J. Geophys. Res.*, 109, D19107. DOI: 10.1029/2004JD004892.

Garcia, R. R., A. K. Smith, D. E. Kinnison, Á. de la Cámara and D. J. Murphy (2017). 'Modification of the Gravity Wave Parameterization in the Whole Atmosphere Community Climate Model: Motivation and Results'. *J. Atmos. Sci.*, 74, pp. 275–291. DOI: 10.1175/JAS-D-16-0104.1.

Gates, W. L., J. S. Boyle, C. Covey, C. G. Dease, C. M. Doutriaux, R. S. Drach, M. Fiorino, P. J. Gleckler, J. J. Hnilo, S. M. Marlais et al. (1999). 'An Overview of the Results of the Atmospheric Model Intercomparison Project (AMIP I)'. *Bull. Am. Meteorol. Soc.*, 80, pp. 29–55. DOI: 10.1175/1520-0477(1999)080<0029:aootro>2.0.co;2.

Gelaro, R., W. McCarty, M. J. Suárez, R. Todling, A. Molod, L. Takacs, C. A. Randles, A. Darmenov, M. G. Bosilovich and R. Reichle (2017). 'The Modern-Era Retrospective Analysis for Research and Applications, Version 2 (MERRA-2)'. *J. Climate*, 30, pp. 5419–5454. DOI: 10.1175/jcli-d-16-0758.1.

Gettelman, A., M. J. Mills, D. E. Kinnison, R. R. Garcia, A. K. Smith, D. R. Marsh, S. Tilmes, F. Vitt, C. G. Bardeen, J. McInerny et al. (2019). 'The Whole Atmosphere Community Climate Model Version 6 (WACCM6)'. *J. Geophys. Res.*, 124, pp. 12380–12403. DOI: 10.1029/2019JD030943.

Gidden, M. J., K. Riahi, S. J. Smith, S. Fujimori, G. Luderer, E. Kriegler, D. P. van Vuuren, M. van den Berg, L. Feng, D. Klein et al. (2019). 'Global emissions pathways under different socioeconomic scenarios for use in CMIP6: a dataset of harmonized emissions trajectories through the end of the century'. *Geosci. Model Dev.*, 12, pp. 1443–1475. DOI: 10.5194/gmd-12-1443-2019.

Giorgetta, M. A., E. Manzini, E. Roeckner, M. Esch and L. Bengtsson (2006). 'Climatology and Forcing of the Quasi-Biennial Oscillation in the MAECHAM5 Model'. *J. Climate*, 19, pp. 3882–3901. DOI: 10.1175/jcli3830.1.

Grell, G. A. and S. R. Freitas (2014). 'A scale and aerosol aware stochastic convective parameterization for weather and air quality modeling'. *Atmos. Chem. Phys.*, 14, pp. 5233–5250. DOI: 10.5194/acp-14-5233-2014.

Hersbach, H., B. Bell, P. Berrisford, S. Hirahara, A. Horányi, J. Muñoz-Sabater, J. Nicolas, C. Peubey, R. Radu, D. Schepers et al. (2020). 'The ERA5 global reanalysis'. *Q. J. R. Meteorol. Soc.*, 146, pp. 1999–2049. DOI: 10.1002/qj.3803.

Hourdin, F., I. Musat, S. Bony, P. Braconnot, F. Codron, J.-L. Dufresne, L. Fairhead, M.-A. Filiberti, P. Friedlingstein, J.-Y. Grandpeix et al. (2006). 'The LMDZ4 general circulation model: climate performance and sensitivity to parametrized physics with emphasis on tropical convection'. *Clim. Dynam.*, 27, pp. 787–813. DOI: 10.1007/s00382-006-0158-0.

Huang, Y., Y. Wang and H. Huang (2020). 'Stratospheric water vapor feedback disclosed by a locking experiment'. *Geophys. Res. Lett.*, 47, e2020GL087987. DOI: 10.1029/2020gl087987.

Huijnen, V., J. Flemming, S. Chabrillat, Q. Errera, Y. Christophe, A.-M. Blechschmidt, A. Richter and H. Eskes (2016). 'C-IFS-CB05-BASCOE: stratospheric chemistry in the Integrated Forecasting System of ECMWF'. *Geosci. Model Dev.*, 9, pp. 3071–3091. DOI: 10.5194/gmd-9-3071-2016.

Hurrell, J. W., M. M. Holland, P. R. Gent, S. Ghan, J. E. Kay, P. J. Kushner, J.-F. Lamarque, W. G. Large, D. Lawrence, K. Lindsay et al. (2013). 'The community Earth system model: A framework for collaborative research'. *Bull. Am. Meteorol. Soc.*, 94, pp. 1339–1360. DOI: 10.1175/BAMS-D-12-00121.1.

Iacono, M. J., J. S. Delamere, E. J. Mlawer, M. W. Shephard, S. A. Clough and W. D. Collins (2008). 'Radiative forcing by long-lived greenhouse gases: Calculations with the AER radiative transfer models'. *J. Geophys. Res.*, 113, D13103. DOI: 10.1029/2008JD009944.

Jöckel, P., A. Kerkweg, A. Pozzer, R. Sander, H. Tost, H. Riede, A. Baumgaertner, S. Gromov and B. Kern (2010). 'Development cycle 2 of the Modular Earth Submodel System (MESSy2)'. *Geosci. Model Dev.*, 3, pp. 717–752. DOI: 10.5194/gmd-3-717-2010.

Jones, A. C., J. M. Haywood, A. Jones and V. Aquila (2016). 'Sensitivity of volcanic aerosol dispersion to meteorological conditions: a Pinatubo case study'. *J. Geophys. Res.*, 121, pp. 6892–6908. DOI: 10.1002/2016JD025001.

Jonsson, A. I., J. de Grandpré, V. I. Fomichev, J. C. McConnell and S. R. Beagley (2004). 'Doubled CO2-induced cooling in the middle atmosphere: Photochemical analysis of the ozone radiative feedback'. *J. Geophys. Res.*, 109, D24103. DOI: 10.1029/2004JD005093.

Jörimann, A., T. Sukhodolov, B. Luo, G. Chiodo, G. Mann and T. Peter (2025). 'REtrieval Method for optical and physical Aerosol Properties in the stratosphere (REMAPv1)'. *Geosci. Model Dev.*, 18, pp. 6023–6041. DOI: 10.5194/gmd-18-6023-2025.

Jörimann, A. (2025). *REMAP-GloSSAC-2023*. Zenodo. DOI: 10.5281/zenodo.14961868.

Kawamiya, M., T. Hajima, K. Tachiiri, S. Watanabe and T. Yokohata (2020). 'Two decades of Earth system modeling with an emphasis on Model for Interdisciplinary Research on Climate (MIROC)'. *Prog. Earth Planet. Sci.*, 7, 64. DOI: 10.1186/s40645-020-00369-5.

Kleinschmitt, C., O. Boucher, S. Bekki, F. Lott and U. Platt (2017). 'The Sectional Stratospheric Sulfate Aerosol module (S3A-v1) within the LMDZ general circulation model: description and evaluation against stratospheric aerosol observations'. *Geosci. Model Dev.*, 10, pp. 3359–3378. DOI: 10.5194/gmd-10-3359-2017.

Kohl, M., C. Brühl, J. Schallock, H. Tost, P. Jöckel, A. Jost, S. Beirle, M. Höpfner and A. Pozzer (2025). 'New submodel for emissions from Explosive Volcanic ERuptions (EVER v1.1) within the Modular Earth Submodel System (MESSy, version 2.55.1)'. *Geosci. Model Dev.*, 18, pp. 3985–4007. DOI: 10.5194/gmd-18-3985-2025.

Kovilakam, M., L. Thomason and T. Knepp (2023). 'SAGE III/ISS aerosol/cloud categorization and its impact on GloSSAC'. *Atmos. Meas. Tech.*, 16, pp. 2709–2731. DOI: 10.5194/amt-16-2709-2023.

Kovilakam, M., L. W. Thomason, N. Ernest, L. Rieger, A. Bourassa and L. Millán (2020). 'The Global Space-based Stratospheric Aerosol Climatology (version 2.0): 1979–2018'. *Earth Syst. Sci. Data*, 12, pp. 2607–2634. DOI: 10.5194/essd-12-2607-2020.

Kuhlbrodt, T., C. G. Jones, A. Sellar, D. Storkey, E. Blockley, M. Stringer, R. Hill, T. Graham, J. Ridley, A. Blaker et al. (2018). 'The Low–Resolution Version of HadGEM3 GC3.1: Development and Evaluation for Global Climate'. *J. Adv. Model. Earth Syst.*, 10, pp. 2865–2888. DOI: 10.1029/2018MS001370.

Lamarque, J.-F., L. K. Emmons, P. G. Hess, D. E. Kinnison, S. Tilmes, F. Vitt, C. L. Heald, E. A. Holland, P. H. Lauritzen, J. Neu et al. (2012). 'CAM-chem: description and evaluation of interactive atmospheric chemistry in the Community Earth System Model'. *Geosci. Model Dev.*, 5, pp. 369–411. DOI: 10.5194/gmd-5-369-2012.

Lefèvre, F., G. P. Brasseur, I. Folkins, A. K. Smith and P. Simon (1994). 'Chemistry of the 1991–1992 stratospheric winter: Three-dimensional model simulations'. *J. Geophys. Res.*, 99, pp. 8183–8195. DOI: 10.1029/93JD03476.

Lefèvre, F., F. Figarol, K. S. Carslaw and T. Peter (1998). 'The 1997 Arctic Ozone depletion quantified from three-dimensional model simulations'. *Geophys. Res. Lett.*, 25, pp. 2425–2428. DOI: 10.1029/98GL51812.

Li, C., Y. Peng, E. Asher, A. A. Baron, M. Todt, T. D. Thornberry, S. Evan, J. Brioude, P. Smale, R. Querel et al. (2024). 'Microphysical Simulation of the 2022 Hunga Volcano Eruption Using a Sectional Aerosol

Model'. *Geophys. Res. Lett.*, 51, e2024GL108522. DOI: 10.1029/2024GL108522.

Lin, S. J. and R. B. Rood (1996). 'Multidimensional flux-form semi-Lagrangian transport schemes'. *Mon. Weather Rev.*, 124, pp. 2046–2070. DOI: 10.1175/1520-0493(1996)124<2046:MFFSLT>2.0.CO;2.

Liu, X., R. C. Easter, S. J. Ghan, R. Zaveri, P. Rasch, X. Shi, J.-F. Lamarque, A. Gettelman, H. Morrison, F. Vitt et al. (2012). 'Toward a minimal representation of aerosols in climate models: description and evaluation in the Community Atmosphere Model CAM5'. *Geosci. Model Dev.*, 5, pp. 709–739. DOI: 10.5194/gmd-5-709-2012.

Liu, X., P.-L. Ma, H. Wang, S. Tilmes, B. Singh, R. C. Easter, S. J. Ghan and P. J. Rasch (2016). 'Description and evaluation of a new four-mode version of the Modal Aerosol Module (MAM4) within version 5.3 of the Community Atmosphere Model'. *Geosci. Model Dev.*, 9, pp. 505–522. DOI: 10.5194/gmd-9-505-2016.

Lock, A. P., A. R. Brown, M. R. Bush, G. M. Martin and R. N. B. Smith (2000). 'A new boundary layer mixing scheme. Part I: Scheme description and single-column model tests'. *Mon. Weather Rev.*, 128, pp. 3187–3199. DOI: 10.1175/1520-0493(2000)128<3187:anblms>2.0.co;2.

Luo, B. (2017). *SAGE-3λ v4: Stratospheric aerosol data for use in CMIP6 models*. ETH Zurich. DOI: 10.3929/ethz-b-000715155.

Lurton, T., Y. Balkanski, V. Bastrikov, S. Bekki, L. Bopp, P. Braconnot, P. Brockmann, P. Cadule, C. Contoux, A. Cozic et al. (2020). 'Implementation of the CMIP6 forcing data in the IPSL-CM6A-LR model'. *J. Adv. Model. Earth Syst.*, 12, e2019MS001940. DOI: 10.1029/2019MS001940.

Mann, G. W., K. S. Carslaw, D. A. Ridley, D. V. Spracklen, K. J. Pringle, J. Merikanto, H. Korhonen, J. P. Schwarz, L. A. Lee, P. T. Manktelow et al. (2012). 'Intercomparison of modal and sectional aerosol microphysics representations within the same 3-D global chemical transport model'. *Atmos. Chem. Phys.*, 12, pp. 4449–4476. DOI: 10.5194/acp-12-4449-2012.

Mann, G. W., K. S. Carslaw, D. V. Spracklen, D. A. Ridley, P. T. Manktelow, M. P. Chipperfield, S. J. Pickering and C. E. Johnson (2010). 'Description and evaluation of GLOMAP-mode: a modal global aerosol microphysics model for the UKCA composition-climate model'. *Geosci. Model Dev.*, 3, pp. 519–551. DOI: 10.5194/gmd-3-519-2010.

Marchand, M., P. Keckhut, S. Lefebvre, C. Claud, D. Cugnet, A. Hauchecorne, F. Lefévre, M.-P. Lefebvre, J. Jumelet, F. Lott et al. (2012). 'Dynamical amplification of the stratospheric solar response simulated with the Chemistry-Climate Model LMDz-Reprobus'. *J. Atmos. Solar-Terr. Phys.*, 75–76, pp. 147–160. DOI: 10.1016/j.jastp.2011.11.008.

Millán, L., M. L. Santee, A. Lambert, N. J. Livesey, F. Werner, M. J. Schwartz, H. C. Pumphrey, G. L. Manney, Y. Wang, H. Su et al. (2022). 'The Hunga Tonga-Hunga Ha'apai Hydration of the Stratosphere'. *Geophys. Res. Lett.*, 49, e2022GL099381. DOI: 10.1029/2022gl099381.

Mills, M. J., J. H. Richter, S. Tilmes, B. Kravitz, D. G. Mac-Martin, A. A. Glanville, J. J. Tribbia, J.-F. Lamarque, F. Vitt, A. Schmidt et al. (2017). 'Radiative and chemical response to interactive stratospheric sulfate aerosols in fully coupled CESM1(WACCM)'. *J. Geophys. Res.*, 122, pp. 13061–13078. DOI: 10.1002/2017JD027006.

Mills, M. J., A. Schmidt, R. Easter, S. Solomon, D. E. Kinnison, S. J. Ghan et al. (2016). 'Global volcanic aerosol properties derived from emissions, 1990–2014, using CESM1 (WACCM)'. *J. Geophys. Res.*, 121, pp. 2332–2348. DOI: 10.1002/2015jd024290.

Mills, M. J., O. B. Toon, V. Vaida, P. E. Hintze, H. G. Kjaergaard, D. P. Schofield and T. W. Robinson (2005). 'Photolysis of sulfuric acid vapor by visible light as a source of the polar stratospheric CN layer'. *J. Geophys. Res.*, 110, D08201. DOI: 10.1029/2004JD005519.

Molod, A., L. Takacs, M. Suarez and J. Bacmeister (2015). 'Development of the GEOS-5 atmospheric general circulation model: evolution from MERRA to MERRA2'. *Geosci. Model Dev.*, 8, pp. 1339–1356. DOI: 10.5194/gmd-8-1339-2015.

Morgenstern, O., P. Braesicke, F. M. O'Connor, A. C. Bushell, C. E. Johnson, S. M. Osprey and J. A. Pyle (2009). 'Evaluation of the new UKCA climate-composition model – Part 1: The stratosphere'. *Geosci. Model Dev.*, 2, pp. 43–57. DOI: 10.5194/gmd-2-43-2009.

Morgenstern, O., M. I. Hegglin, E. Rozanov, F. M. O'Connor, N. L. Abraham, H. Akiyoshi, A. T. Archibald, S. Bekki, N. Butchart, M. P. Chipperfield et al. (2017). 'Review of the global models used within phase 1 of the Chemistry–Climate Model Initiative (CCMI)'. *Geosci. Model Dev.*, 10, pp. 639–671. DOI: 10.5194/gmd-10-639-2017.

Mulcahy, J. P., C. Jones, A. Sellar, B. Johnson, I. A. Boutle, A. Jones, T. Andrews, S. T. Rumbold, J. Mollard, N. Bellouin et al. (2018). 'Improved Aerosol Processes and Effective Radiative Forcing in HadGEM3 and UKESM1'. *J. Adv. Model. Earth Syst.*, 10, pp. 2786–2805. DOI: 10.1029/2018MS001464.

Mulcahy, J. P., C. Johnson, C. G. Jones, A. C. Povey, C. E. Scott, A. Sellar, S. T. Turnock, M. T. Woodhouse, N. L. Abraham, M. B. Andrews et al. (2020). 'Description and evaluation of aerosol in UKESM1 and HadGEM3-GC3.1 CMIP6 historical simulations'. *Geosci. Model Dev.*, 13, pp. 6383–6423. DOI: 10.5194/gmd-13-6383-2020.

Mulcahy, J. P., C. G. Jones, S. T. Rumbold, T. Kuhlbrodt, A. J. Dittus, E. W. Blockley, A. Yool, J. Walton, C. Hardacre, T. Andrews et al. (2023). 'UKESM1.1: development and evaluation of an updated configuration of the UK Earth System Model'. *Geosci. Model Dev.*, 16, pp. 1569–1600. DOI: 10.5194/gmd-16-1569-2023.

Naujokat, B. (1986). 'An update of the observed Quasi-Biennial Oscillation of the stratospheric winds over the tropics'. *J. Atmos. Sci.*, 43, pp. 1873–1877. DOI: 10.1175/1520-0469(1986)043<1873:AUOTOQ>2.0.CO;2.

Neely III, R. R. and A. Schmidt (2016). *VolcanEESM: Global volcanic sulphur dioxide (SO_2) emissions database from 1850 to present.* Centre for Environmental Data Analysis. DOI: 10.5285/76ebdc0b-0eed-4f70-b89e-55e606bcd568.

Nielsen, J. E., S. Pawson, A. Molod, B. Auer, A. M. da Silva, A. R. Douglass, B. Duncan, Q. Liang, M. Manyin, L. D. Oman et al. (2017). 'Chemical mechanisms and their applications in the Goddard Earth Observing System (GEOS) earth system model'. *J. Adv. Model. Earth Syst.*, 9, pp. 3019–3044. DOI: 10.1002/2017MS001011.

O'Connor, F. M., C. E. Johnson, O. Morgenstern, N. L. Abraham, P. Braesicke, M. Dalvi, G. A. Folberth, M. G. Sanderson, P. J. Telford, A. Voulgarakis et al. (2014). 'Evaluation of the new UKCA climate-composition model – Part 2: The Troposphere'. *Geosci. Model Dev.*, 7, pp. 41–91. DOI: 10.5194/gmd-7-41-2014.

O'Neill, B. C., C. Tebaldi, D. P. van Vuuren, V. Eyring, P. Friedlingstein, G. Hurtt, R. Knutti, E. Kriegler, J.-F. Lamarque, J. Lowe et al. (2016). 'The Scenario Model Intercomparison Project (ScenarioMIP) for CMIP6'. *Geosci. Model Dev.*, 9, pp. 3461–3482. DOI: 10.5194/gmd-9-3461-2016.

Peuch, V.-H., R. Engelen, M. Rixen, D. Dee, J. Flemming, M. Suttie, M. Ades, A. Agusti-Panareda, C. Ananasso, E. Andersson et al. (2022). 'The Copernicus Atmosphere Monitoring Service: From Research to Operations'. *Bull. Am. Meteorol. Soc.*, 103, E2650–E2668. DOI: 10.1175/BAMS-D-21-0314.1.

Pringle, K. J., H. Tost, S. Message, B. Steil, D. Giannadaki, A. Nenes, C. Fountoukis, P. Stier, E. Vignati and J. Lelieveld (2010). 'Description and evaluation of GMXe: a new aerosol submodel for global simulations (v1)'. *Geosci. Model Dev.*, 3, pp. 391–412. DOI: 10.5194/gmd-3-391-2010.

Putman, W. M. and S.-J. Lin (2007). 'Finite-volume transport on various cubed-sphere grids'. *J. Comput. Phys.*, 227, pp. 55–78. DOI: 10.1016/j.jcp.2007.07.022.

Quaglia, I., C. Timmreck, U. Niemeier, D. Visioni, G. Pitari, C. Brodowsky, C. Brühl, S. S. Dhomse, H. Franke, A. Laakso et al. (2023). 'Interactive stratospheric aerosol models' response to different amounts and altitudes of SO_2 injection during the 1991 Pinatubo eruption'. *Atmos. Chem. Phys.*, 23, pp. 921–948. DOI: 10.5194/acp-23-921-2023.

Randel, W. J., X. Wang, J. Starr, R. R. Garcia and D. Kinnison (2024). 'Long-Term Temperature Impacts of the Hunga Volcanic Eruption in the Stratosphere and Above'. *Geophys. Res. Lett.*, 51. DOI: 10.1029/2024gl111500.

Reinecker, M., M. Suarez, R. Todling, J. Bacmeister, L. Takacs and H. Liu (2008). *The GEOS-5 Data Assimilation System: Documentation of Versions 5.0.1, 5.1.0.* Tech. rep. NASA Technical Report TM-2007-104606.

Rémy, S., Z. Kipling, V. Huijnen, J. Flemming, P. Nabat, M. Michou, M. Ades, R. Engelen and V.-H. Peuch (2022). 'Description and evaluation of the tropospheric aerosol scheme in the Integrated Forecasting System (IFS-AER, cycle 47R1) of ECMWF'. *Geosci. Model Dev.*, 15, pp. 4881–4912. DOI: 10.5194/gmd-15-4881-2022.

Reynolds, R. W., N. A. Rayner, T. M. Smith, D. C. Stokes and W. Wang (2002). 'An Improved In Situ and Satellite SST Analysis for Climate'. *J. Climate*, 15, pp. 1609–1625. DOI: 10.1175/1520-0442(2002)015<1609:AIISAS>2.0.CO;2.

Schallock, J., C. Brühl, C. Bingen, M. Höpfner, L. Rieger and J. Lelieveld (2023). 'Reconstructing volcanic radiative forcing since 1990, using a comprehensive emission inventory and spatially resolved sulfur injections from satellite data in a chemistry-

climate model'. *Atmos. Chem. Phys.*, 23, pp. 1169–1207. DOI: 10.5194/acp-23-1169-2023.

Scinocca, J. F. (2003). 'An Accurate Spectral Non-Orographic Gravity Wave Parameterization for General Circulation Models'. *J. Atmos. Sci.*, 60, pp. 667–682. DOI: 10.1175/1520-0469(2003)060<0667:AASNGW>2.0.CO;2.

Scinocca, J. F., N. A. McFarlane, M. Lazare, J. Li and D. Plummer (2008). 'Technical Note: The CCCma third generation AGCM and its extension into the middle atmosphere'. *Atmos. Chem. Phys.*, 8, pp. 7055–7074. DOI: 10.5194/acp-8-7055-2008.

Seddon, J., A. Stephens, M. S. Mizielinski, P. L. Vidale and M. J. Roberts (2023). 'Technology to aid the analysis of large-volume multi-institute climate model output at a central analysis facility (PRIMAVERA Data Management Tool V2.10)'. *Geosci. Model Dev.*, 16, pp. 6689–6700. DOI: 10.5194/gmd-16-6689-2023.

Sekiya, T., K. Sudo and T. Nagai (2016). 'Evolution of stratospheric sulfate aerosol from the 1991 Pinatubo eruption: Roles of aerosol microphysical processes'. *J. Geophys. Res.*, 121, pp. 2911–2938. DOI: 10.1002/2015JD024313.

Sellar, A. A., C. G. Jones, J. P. Mulcahy, Y. Tang, A. Yool, A. Wiltshire, F. M. O'Connor, M. Stringer, R. Hill, J. Palmieri et al. (2019). 'UKESM1: Description and Evaluation of the U.K. Earth System Model'. *J. Adv. Model. Earth Syst.*, 11, pp. 4513–4558. DOI: 10.1029/2019MS001739.

Sellar, A. A., J. Walton, C. G. Jones, R. Wood, N. L. Abraham, M. Andrejczuk, M. B. Andrews, T. Andrews, A. T. Archibald, L. de Mora et al. (2020). 'Implementation of U.K. Earth System Models for CMIP6'. *J. Adv. Model. Earth Syst.*, 12, e2019MS001946. DOI: 10.1029/2019MS001946.

Sellitto, P., A. Podglajen, R. Belhadji, M. Boichu, E. Carboni, J. Cuesta, C. Duchamp, C. Kloss, R. Siddans, N. Bègue et al. (2022). 'The unexpected radiative impact of the Hunga Tonga eruption of 15th January 2022'. *Commun. Earth Environ.*, 3, 288. DOI: 10.1038/s43247-022-00618-z.

SPARC (2010). *SPARC CCMVal Report on the Evaluation of Chemistry-Climate Models*. Tech. rep. https://www.aparc-climate.org/publications/sparc-reports/sparc-report-no-5/. SPARC Report No. 5, WCRP-30/2010, WMO/TD-No. 40.

Strahan, S. E., B. N. Duncan and P. Hoor (2007). 'Observationally derived transport diagnostics for the lowermost stratosphere and their application to the GMI chemistry and transport model'. *Atmos. Chem. Phys.*, 7, pp. 2435–2445. DOI: 10.5194/acp-7-2435-2007.

Sukhodolov, T., T. Egorova, A. Stenke, W. T. Ball, C. Brodowsky, G. Chiodo, A. Feinberg, M. Friedel, A. Karagodin-Doyennel, T. Peter et al. (2021). 'Atmosphere ocean aerosol chemistry climate model SOCOLv4.0: description and evaluation'. *Geosci. Model Dev.*, 14, pp. 5525–5560. DOI: 10.5194/gmd-14-5525-2021.

Taha, G., R. Loughman, P. R. Colarco, T. Zhu, L. W. Thomason and G. Jaross (2022). 'Tracking the 2022 Hunga Tonga-Hunga Ha'apai Aerosol Cloud in the Upper and Middle Stratosphere Using Space-Based Observations'. *Geophys. Res. Lett.*, 49, e2022GL100091. DOI: 10.1029/2022gl100091.

Taha, G., R. Loughman, T. Zhu, L. Thomason, J. Kar, L. Rieger and A. Bourassa (2021). 'OMPS LP Version 2.0 multi-wavelength aerosol extinction coefficient retrieval algorithm'. *Atmos. Meas. Tech.*, 14, pp. 1015–1036. DOI: 10.5194/amt-14-1015-2021.

Tatebe, H., T. Ogura, T. Nitta, Y. Komuro, K. Ogochi, T. Takemura, K. Sudo, M. Sekiguchi, M. Abe, F. Saito et al. (2019). 'Description and basic evaluation of simulated mean state, internal variability, and climate sensitivity in MIROC6'. *Geosci. Model Dev.*, 12, pp. 2727–2765. DOI: 10.5194/gmd-12-2727-2019.

Telford, P., P. Braesicke, O. Morgenstern and J. Pyle (2009). 'Reassessment of causes of ozone column variability following the eruption of Mount Pinatubo using a nudged CCM'. *Atmos. Chem. Phys.*, 9, pp. 4251–4260. DOI: 10.5194/acp-9-4251-2009.

Telford, P. J., P. Braesicke, O. Morgenstern and J. A. Pyle (2008). 'Technical Note: Description and assessment of a nudged version of the new dynamics Unified Model'. *Atmos. Chem. Phys.*, 8, pp. 1701–1712. DOI: 10.5194/acp-8-1701-2008.

Thomason, L. W., N. Ernest, L. Millán, L. Rieger, A. Bourassa, J.-P. Vernier, G. Manney, B. Luo, F. Arfeuille and T. Peter (2018). 'A global space-based stratospheric aerosol climatology: 1979–2016'. *Earth Syst. Sci. Data*, 10, pp. 469–492. DOI: 10.5194/essd-10-469-2018.

Tilmes, S., M. J. Mills, Y. Zhu, C. G. Bardeen, F. Vitt, P. Yu, D. Fillmore, X. Liu, B. Toon and T. Deshler (2023). 'Description and performance of a sectional aerosol microphysical model in the Community Earth System Model (CESM2)'. *Geosci. Model Dev.*, 16, pp. 6087–6125. DOI: 10.5194/gmd-16-6087-2023.

Tsujino, H., S. Urakawa, H. Nakano, R. J. Small, W. M. Kim, S. G. Yeager, G. Danabasoglu, T. Suzuki, J. L. Bamber, M. Bentsen et al. (2018). 'JRA-55 based surface dataset for driving ocean–sea-ice models (JRA55-do)'. *Ocean Model.*, 130, pp. 79–139. DOI: 10.1016/j.ocemod.2018.07.002.

Vehkamäki, H., M. Kulmala, I. Napari, K. E. Lehtinen, C. Timmreck, M. Noppel and A. Laaksonen (2002). 'An improved parameterization for sulfuric acid-water nucleation rates for tropospheric and stratospheric conditions'. *J. Geophys. Res.*, 107, AAC3-1–AAC3-10. DOI: 10.1029/2002JD002184.

Walters, D., A. J. Baran, I. Boutle, M. Brooks, P. Earnshaw, J. Edwards, K. Furtado, P. Hill, A. Lock, J. Manners et al. (2019). 'The Met Office Unified Model Global Atmosphere 7.0/7.1 and JULES Global Land 7.0 configurations'. *Geosci. Model Dev.*, 12, pp. 1909–1963. DOI: 10.5194/gmd-12-1909-2019.

Wang, X. (2025). *MLS H2O anomaly 2022*. Zenodo. DOI: 10.5281/zenodo.14962954.

Wang, X., W. Randel, Y. Zhu, S. Tilmes, J. Starr, W. Yu, R. Garcia, O. B. Toon, M. Park, D. Kinnison et al. (2023). 'Stratospheric Climate Anomalies and Ozone Loss Caused by the Hunga Tonga-Hunga Ha'apai Volcanic Eruption'. *J. Geophys. Res.*, 128, e2023JD039480. DOI: 10.1029/2023jd039480.

Watanabe, S., T. Hajima, K. Sudo, T. Nagashima, T. Takemura, H. Okajima, T. Nozawa, H. Kawase, M. Abe, T. Yokohata et al. (2011). 'MIROC-ESM 2010: model description and basic results of CMIP5-20c3m experiments'. *Geosci. Model Dev.*, 4, pp. 845–872. DOI: 10.5194/gmd-4-845-2011.

Williams, J. E., V. Huijnen, I. Bouarar, M. Meziane, T. Schreurs, S. Pelletier, V. Marécal, B. Josse and J. Flemming (2022). 'Regional evaluation of the performance of the global CAMS chemical modeling system over the United States (IFS cycle 47r1)'. *Geosci. Model Dev.*, 15, pp. 4657–4687. DOI: 10.5194/gmd-15-4657-2022.

Williams, K. D., D. Copsey, E. W. Blockley, A. Bodas-Salcedo, D. Calvert, R. Comer, P. Davis, T. Graham, H. T. Hewitt, R. Hill et al. (2018). 'The Met Office Global Coupled Model 3.0 and 3.1 (GC3.0 and GC3.1) Configurations'. *J. Adv. Model. Earth Syst.*, 10, pp. 357–380. DOI: 10.1002/2017MS001115.

Wood, N., A. Staniforth, A. White, T. Allen, M. Diamantakis, M. Gross, T. Melvin, C. Smith, S. Vosper, M. Zerroukat et al. (2014). 'An inherently mass-conserving semi-implicit semi-Lagrangian discretization of the deep-atmosphere global non-hydrostatic equations'. *Q. J. R. Meteorol. Soc.*, 140, pp. 1505–1520. DOI: 10.1002/qj.2235.

Yu, P., O. B. Toon, C. G. Bardeen, M. J. Mills, T. Fan, J. M. English and R. R. Neely (2015). 'Evaluations of tropospheric aerosol properties simulated by the Community Earth System Model with a sectional aerosol microphysics scheme'. *J. Adv. Model. Earth Syst.*, 7, pp. 865–914. DOI: 10.1002/2014MS000421.

Yu, W., R. Garcia, J. Yue, A. Smith, X. Wang, W. Randel, Z. Qiao, Y. Zhu, V. L. Harvey, S. Tilmes et al. (2023). 'Mesospheric temperature and circulation response to the Hunga Tonga-Hunga-Ha'apai volcanic eruption'. *J. Geophys. Res.*, 128, e2023JD039636. DOI: 10.1029/2023JD039636.

Zhang, J., D. Kinnison, Y. Zhu, X. Wang, S. Tilmes, K. Dube and W. Randel (2024). 'Chemistry Contribution to Stratospheric Ozone Depletion After the Unprecedented Water-Rich Hunga Tonga Eruption'. *Geophys. Res. Lett.*, 51, e2023GL105762. DOI: 10.1029/2023gl105762.

Zhou, X., S. S. Dhomse, W. Feng, G. Mann, S. Heddell, H. Pumphrey, B. J. Kerridge, B. Latter, R. Siddans, L. Ventress et al. (2024). 'Antarctic Vortex Dehydration in 2023 as a Substantial Removal Pathway for Hunga Tonga-Hunga Ha'apai Water Vapor'. *Geophys. Res. Lett.*, 51, e2023GL107630. DOI: 10.1029/2023gl107630.

Zhu, Y., H. Akiyoshi, V. Aquila, E. Asher, E. M. Bednarz, S. Bekki, C. Brühl, A. H. Butler, P. Case, S. Chabrillat et al. (2025). 'Hunga Tonga–Hunga Ha'apai Volcano Impact Model Observation Comparison (HTHH-MOC) project: experiment protocol and model descriptions'. *Geosci. Model Dev.*, 18, pp. 5487–5512. DOI: 10.5194/gmd-18-5487-2025.

Zhu, Y., C. G. Bardeen, S. Tilmes, M. J. Mills, X. Wang, V. L. Harvey, G. Taha, D. Kinnison, R. W. Portmann, P. Yu et al. (2022). 'Perturbations in stratospheric aerosol evolution due to the water-rich plume of the 2022 Hunga-Tonga eruption'. *Commun. Earth Environ.*, 3, 248. DOI: 10.1038/s43247-022-00580-w.

Zhuo, Z., X. Wang, Y. Zhu, W. Yu, E. M. Bednarz, E. Fleming, P. R. Colarco, S. Watanabe, D. Plummer, G. Stenchikov et al. (2025). 'Comparing multimodel ensemble simulations with observations and decadal projections of upper atmospheric variations following the Hunga eruption'. *Atmos. Chem. Phys.*, 25, pp. 13161–13176. DOI: 10.5194/acp-25-13161-2025.